Identification of Surrogate Biomarkers for the Replacement Histopathological Growth Pattern in Colorectal Cancer Liver Metastasis

Vincent Palmieri

Division of Experimental Medicine
McGill University, Montreal, Canada

April 2019

A thesis submitted to McGill University in partial fulfillment of the requirements for the degree of Master of Science in Experimental Medicine.

Table of Contents

Abstract

Introduction

Colorectal cancer (CRC) is the third most common cancer in both males and females in North America. It is the second leading cause of cancer-related deaths due in large part to CRC liver metastasis (CRCLM), with which approximately 50% of patients will be diagnosed during the course of their disease. Three major histopathological growth patterns (HGP) have been identified in CRCLM, and evidence suggests that the tumour's predominant HGP has prognostic implications. Specifically, CRCLMs that present with the replacement growth pattern are resistant to anti-angiogenic therapy, which is frequently used alongside neoadjuvant chemotherapy for the treatment of metastatic CRC. The HGPs in CRCLM may have a promising role as predictive biomarkers of response to angiogenesis inhibitors, where no such marker has yet been validated. However, a CRCLM's growth pattern must be evaluated by a pathologist from resected tumour tissue, implying that preoperative treatment precedes HGP scoring. Therefore, surrogate molecular markers for the CRCLM HGPs that can be assessed prior to surgery would be instrumental in determining whether a patient may benefit from anti-angiogenic treatment.

Objectives

It is hypothesized that there are products of differentially expressed genes (DEG) in replacement HGP CRCLMs that may serve as potential diagnostic biomarkers and/or targets for anti-metastatic therapy. The objective of this study is to characterize and compare the global gene expression profiles of chemonaïve CRCLMs presenting with the replacement or desmoplastic HGPs via RNA sequencing (RNA-Seq) and immunohistochemical staining. The secondary aim is to isolate extracellular vesicles (EV) from the plasma of CRCLM patients and verify whether they contain the gene products of select DEGs.

Methods

RNA-Seq was performed using the total RNA extracted from liver metastases and adjacent normal liver tissues that had been resected from 18 patients with CRCLM who did not receive preoperative chemotherapy. Immunohistochemical staining of select DEGs identified from the RNA-Seq data, among other protein targets, was then performed on formalin-fixed, paraffin-

embedded (FFPE) CRCLM samples. The visualization and analysis of immunohistochemistry results were done using the Aperio ImageScope software program. Lastly, EVs were isolated from patient plasma samples by differential centrifugation and subsequently lysed for protein detection via Western blot.

Results

A gene expression signature comprised of genes whose transcription was upregulated in chemonaïve replacement HGP CRCLMs compared to chemonaïve desmoplastic HGP CRCLMs and normal liver tissues was generated. The protein levels of one of these genes, LOXL4, were found to be significantly elevated at the tumour-liver interface and in areas of inflammation in replacement HGP metastases. LOXL4 protein was also detectable in EVs isolated from the plasma of patients with CRCLM or benign liver disease, though the quantities were comparable between the growth patterns.

Conclusion

Our study showed that the replacement and desmoplastic HGP CRCLMs have distinguishable gene expression profiles, with several genes related to the extracellular matrix and the immune system being upregulated in replacement HGP metastases. The expression levels of LOXL4 mRNA and protein were significantly elevated in replacement HGP CRCLMs relative to desmoplastic HGP CRCLMs, and LOXL4 protein is also detectable in EVs isolated from patient plasma. Therefore, LOXL4 may potentially serve as a surrogate biomarker for the replacement HGP in CRCLM.

Résumé

Introduction

Le cancer colorectal (CCR) est le troisième cancer le plus fréquent chez les hommes et les femmes en Amérique du Nord. Il s'agit de la deuxième principale cause de décès liés au cancer, en grande partie à cause des métastases hépatiques du CCR (MHCCR), avec lesquelles environ 50% des patients recevront un diagnostic au cours de leur maladie. Trois modèles de croissance histopathologique (HGP) ont été identifiés dans les MHCCR, et les preuves suggèrent que le HGP prédominant de la tumeur pourrait avoir des implications pronostiques. Plus précisément, les MHCCR qui présentent un HGP de remplacement sont résistantes aux inhibiteurs de l'angiogenèse, qui sont souvent administrés en association avec la chimiothérapie néoadjuvante pour le traitement du CCR métastatique. Les HGPs pourraient ainsi jouer un rôle en tant que biomarqueurs prédictifs de la réponse au traitement anti-angiogénique. Cependant, le HGP d'une MHCCR doit être évalué par un pathologiste à partir de tissus tumoraux réséqués, ce qui implique que le traitement préopératoire précède la cotation du HGP. Par conséquent, des marqueurs moléculaires de substitution pour les HGPs qui peuvent être évalués avant l'intervention chirurgicale seraient utiles pour déterminer si un patient peut bénéficier d'un traitement anti-angiogénique.

Objectifs

On suppose qu'il existe des produits géniques de gènes différemment exprimés (DEG) dans les MHCCR avec le HGP de remplacement qui peuvent servir de biomarqueurs diagnostics ou de cibles pour le traitement anti-métastatique. L'objectif de cette étude est de caractériser et de comparer les profils d'expression génique des MHCCR présentant le HGP de remplacement ou de desmoplasie via le séquençage de l'ARN (RNA-Seq) et l'immunohistochimie. L'objectif secondaire est d'isoler les vésicules extracellulaires (EV) du plasma des patients atteints de MHCCR et de vérifier si elles contiennent les produits géniques de DEG entre les HGPs.

Méthodes

RNA-Seq a été effectué en utilisant l'ARN total extrait des métastases hépatiques et des tissus hépatiques normaux qui avaient été prélevés chez 18 patients atteints de MHCCR qui

n’avaient pas reçu de chimiothérapie préopératoire. La coloration histochimique de certains produits géniques identifiés à partir des données du RNA-Seq, entre autres cibles protéiques, a ensuite été effectuée sur des échantillons de MHCCR. La visualisation et l’analyse des résultats de l’immunohistochimie ont été réalisées à l’aide du logiciel Aperio ImageScope. Enfin, les EVs ont été isolées à partir d’échantillons de plasma de patients par centrifugation différentielle, puis lysées pour la détection des protéines par western blot.

Résultats

Une signature d’expression génique composée de gènes dont la transcription était régulée à la hausse dans les MHCCR avec le HGP de remplacement par rapport à celles avec le HGP de desmoplasie et aux tissues hépatiques normaux a été générée. Les taux de protéines de l’un de ces gènes, LOXL4, ont été significativement élevés à l’interface tumeur-foie et dans les zones d’inflammation dans les métastases avec le HGP de remplacement. La protéine LOXL4 était également détectable dans les EVs isolées du plasma de patients atteints de MHCCR ou d’une maladie hépatique bénigne, bien que les quantités étaient comparables entre les HGPs.

Conclusion

Notre étude a montré que les MHCCR avec les HGPs de remplacement et de desmoplasie ont des profils d’expression génique distincts, avec plusieurs gènes liés à la matrice extracellulaire et le système immunitaire étant régulés à la hausse dans les tumeurs présentant le HGP de remplacement. Les niveaux d’expression de l’ARN et de la protéine LOXL4 étaient significativement élevés dans les MHCCR avec le HGP de remplacement, et la protéine LOXL4 était également détectable dans les EVs isolées du plasma des patients. Par conséquent, LOXL4 peut potentiellement servir de biomarqueur de substitution pour le HGP de remplacement dans les MHCCR.

Acknowledgements

I am immeasurably grateful for the numerous individuals whose support and guidance have profoundly contributed to my completion of this chapter of my academic career.

I would like to dedicate my first expression of gratitude to my parents, sister, and other family members who continue to provide me with their endless encouragement in my various pursuits. This work, among other endeavours, would not be possible without their presence.

Many thanks to Dr. Anthoula Lazaris who guided me through a multitude of procedures during my graduate studies, from experimental planning to grant writing. Her knowledge, experience, and generosity with her time were truly invaluable.

I want to thank Abdellatif Amri and Stephanie Petrillo, whose expertise in laboratory techniques and biobanking were essential in my research. Their patience and willingness to help made my time at the bench more productive and enjoyable.

I am grateful for the other members of the Metrakos lab with whom I had the great pleasure of interacting – Hussam, Ayat, Tony, Khaloud, Audrey, Nisreen, Balqis, Rafif, and Miran. This experience was all the more an enriching one having shared it with a group of motivated and uplifting students.

I must also acknowledge the aid and advice I have received from select individuals in neighbouring research teams at the RI-MUHC, namely those under the supervision of Dr. Miguel Burnier and Dr. Janusz Rak. Specifically, the contributions from Dr. Pablo Zoroquiain, Dr. Bia Dias, Dr. Dongsic Choi, and Dr. Laura Montermini were critical for the realization of my work. Similarly, special thanks are owed to Dr. Zu-hua Gao and Dr. Woong-Yang Park for the pathologic scoring and RNA sequencing of our CRCLM samples, respectively. Likewise, I am grateful for the members of my Thesis Committee – Dr. Maxime Bouchard, Dr. Peter Siegel, and my co-supervisor, Dr. Morag Park, whose feedback was highly valued.

Finally, I would like to express my most sincere appreciation for my supervisor, Dr. Peter Metrakos. This work was made achievable by his ongoing support and mentorship, and I thank him for strongly reinforcing my passion for research and ambition to become a clinician scientist.

List of Figures and Tables

Abbreviations

5-FU	5-fluorouracil
Ab	Antibody
BAPN	ß-aminoproprionitrile
Bev-chemo	Bevacizumab plus chemotherapy
BMDC	Bone marrow-derived cell
CD11b	Cluster of differentiation 11b
CD68	Cluster of differentiation 68
CD81	Cluster of differentiation 81
CRC	Colorectal cancer
CRCLM	Colorectal cancer liver metastasis
CT	Computed tomography
CXCL6	Chemokine (C-X-C motif) ligand 6
DAB	3,3′-Diaminobenzidine
DAPI	4′,6-diamidino-2-phenylindole
DEG	Differentially expressed gene
DHGP	Desmoplastic histopathological growth pattern
DN	Desmoplastic histopathological growth pattern – adjacent normal liver
DR	Desmoplastic ring
DT	Desmoplastic histopathological growth pattern – tumour
ECM	Extracellular matrix
EGFR	Epidermal growth factor receptor
EpCAM	Epithelial cell adhesion molecule
ER$^-$	Estrogen receptor-negative
ERK	Extracellular signal-regulated kinase
EV	Extracellular vesicle
FAK	Focal adhesion kinase
FFPE	Formalin-fixed, paraffin-embedded
FLR	Future liver remnant

FOBT	Fecal occult blood test
H&E	Hematoxylin and eosin
HCC	Hepatocellular carcinoma
Hep Par-1	Hepatocyte specific antigen
HGP	Histopathological growth pattern
HNSCC	Head and neck squamous cell carcinoma
HRP	Horseradish peroxidase
IBD	Inflammatory bowel disease
IF	Immunofluorescence
IHC	Immunohistochemistry
LOX	Lysyl oxidase
LOXL1-4	Lysyl oxidase-like 1-4
Lv	Normal liver parenchyma
mAb	Monoclonal antibody
MMP-2	Matrix metalloproteinase-2
MUHC	McGill University Health Centre
NTA	Nanoparticle tracking analysis
PBS	Phosphate-buffered saline
PBS-T	Phosphate-buffered saline with Tween-20
PVE	Portal vein embolization
RANKL	Receptor activator of nuclear factor kappa-B ligand
RCT	Randomized controlled trial
RHGP	Replacement histopathological growth pattern
RI-MUHC	Research Institute of the McGill University Health Centre
RN	Replacement histopathological growth pattern – adjacent normal liver
RNA-Seq	RNA sequencing
RT	Replacement histopathological growth pattern – tumour
SCID	Severe combined immunodeficiency
SDS-PAGE	Sodium dodecyl sulfate–polyacrylamide gel electrophoresis
SRCR	Scavenger receptor cysteine-rich
TAPA-1	Target of antiproliferative antibody 1

TBS-T	Tris-buffered saline with Tween-20
TGF-ß1	Transforming growth factor beta 1
TNC	Tenascin C
TNM	Tumour, node, metastasis
TSG101	Tumour susceptibility gene 101
VEGF-A	Vascular endothelial growth factor A
VIM	Vimentin

Chapter 1: Literature Review

1.1. **Colorectal cancer**

1.1.1. Overview and epidemiology

Colorectal cancer (CRC) is the third most commonly diagnosed type of cancer in both males and females in North America, and is the second leading cause of cancer-related deaths [1,2]. Approximately 90% of new CRC cases occur in individuals aged 50 years or older, though the incidence and mortality rates for these patients have been decreasing over the past decades. These improving trends are likely attributable to a variety of factors, such as the development of better treatments, the implementation of screening programs, and changes in behaviours associated with CRC risk [3]. Conversely, the incidence rates for individuals younger than 50 years of age have been gradually increasing during this time, despite them accounting for a minority of CRC cases [1,3].

Most CRC cases presumably result from the interplay between numerous risk factors, which in addition to older age and male sex, include family history of CRC, inflammatory bowel disease (IBD), diabetes, smoking, alcohol consumption, obesity, and the consumption of red and processed meat. Contrarily, epidemiological studies have also identified several preventative factors like physical activity, aspirin, and the use of hormonal replacement therapy. Lastly, a significant heritable component has been well-established in CRC, with select twin studies suggesting that over one third of cases may be derived from hereditary factors [4].

1.1.2. Clinical presentation, diagnosis, and staging

While CRCs may produce a variety of signs and symptoms, many are non-specific and tend to become more noticeable only in advanced stages of disease. Similar to other lower gastrointestinal conditions, CRCs can present with abdominal pain, changes in bowel habits, rectal bleeding, nausea, vomiting, weakness, malaise, and involuntary weight loss. Symptom occurrence and severity largely depend on the location and size of the tumour, as well as its invasiveness and potential to metastasize [5]. Clinical features that should increase suspicion for CRC are iron deficiency anemia of undetermined cause, hypoalbuminemia from malnutrition, and the presence of any palpable abdominal or rectal mass [6].

Provided sufficient clinical suspicion on the account of signs, symptoms, and laboratory tests, a definitive diagnosis of CRC can be made by the histological examination of biopsies taken during colonoscopy. If colonoscopy is contraindicated because of major comorbidities, flexible sigmoidoscopy plus barium enema or computed tomographic (CT) colonography may serve as alternate means of obtaining a diagnosis [7,8].

The tumour, node, metastasis (TNM) classification system is used to stage CRC. The assessment of each category is based on findings from physical examination, imaging studies, and surgical exploration. Endoscopy is also particularly important when evaluating the primary tumour category. This category reflects the degree to which the primary tumour has invaded the layers of the gastrointestinal wall and/or surrounding tissues. The node category is representative of the number of regional lymph nodes that have detectable metastatic disease. The metastasis category indicates whether any distant metastases have developed. A stage is finally assigned to a CRC by combining these three classifications [9].

1.1.3. Management

A multidisciplinary team is required for the optimal management of a patient with CRC. Surgery, radiotherapy, and chemotherapy play a role in treatment on a case-by-case basis. Both cancer- and patient-related factors must be considered when offering treatment modalities, such as the tumour's stage and anatomic location, and the individual's performance status and comorbidities [4,7].

Surgical excision of the tumour by open or laparoscopic resection constitutes the typical treatment of stage I CRC. Neither neoadjuvant nor adjuvant therapy should be necessary if stage I disease is removed with negative resection margins due to low local recurrence rates [4,7]. However, some studies have reported that patients with stage III CRC who received neoadjuvant radiotherapy or combined chemoradiotherapy benefitted from reduced post-operative rates of local recurrence [10,11]. Patients with high-risk stage II or stage III disease also benefit from adjuvant chemotherapy. The choice of first-line regimen should be made following the clinical evaluation of the patient and a thorough discussion that touches upon patient preferences and potential adverse effects, among other topics. Chemotherapy regimens containing either 5-fluorouracil (5-FU) or capecitabine, in

addition to oxaliplatin, have been shown to improve recurrence and overall survival rates in randomized controlled trials (RCT) [12,13].

1.1.4. Screening

An estimated 80% of CRCs develop from adenomatous polyps through a process known as the adenoma-carcinoma sequence. This multistep transformation results from the accumulation of well-characterized mutations including those of the APC, KRAS, and TP53 genes, which occurs over many years. Consequently, there is an opportunity to detect and remove these polyps before they can possibly progress to CRCs [14].

Current guidelines recommend that programmatic screening for adenomatous polyps and CRC should be offered to individuals at average risk beginning from the age of 50 years, and conclude at the age of 75 years [15]. There are multiple screening options: fecal occult blood test (FOBT), flexible sigmoidoscopy, double-contrast barium enema, colonoscopy, CT colonography, and fecal DNA testing. However, some of these modalities lack RCT evidence of conferring mortality benefits to date [16]. The reviewed guidelines on CRC screening published by the Canadian Association of Gastroenterology in 2010 recommend either FOBT or flexible sigmoidoscopy for population-based screening. Immunochemical FOBT is preferred to the guaiac-based test, and the suggested interval between flexible sigmoidoscopies is at least 10 years [15].

Individuals who have at least one first-degree relative with CRC, long-standing IBD, familial adenomatous polyposis, or Lynch syndrome constitute the high risk groups. The starting age and subsequent intervals for CRC screening in these cases are dependent on the patient's particular hereditary condition and/or family history [17].

1.2. **Colorectal cancer liver metastasis**

1.2.1. Overview and management

Metastatic disease of the liver develops in greater than 50% of patients with CRC, and CRC liver metastasis (CRCLM) is the principal cause of cancer-related death in these individuals. Approximately half the cases of CRCLM will be detectable upon presentation of the primary tumour by standard imaging modalities, whereas the rest may arise months or years after the patient is diagnosed with CRC [18].

Surgical resection is the most effective treatment for CRCLM; five-year overall survival rates have exceeded 50% in multiple studies, and 10-year survivorship is becoming less uncommon in patients with resected metastases [19,20]. However, only 10% to 20% of patients who have CRCLM present with disease that is deemed resectable. Therefore, advances have been made in systemic chemotherapy as well as in techniques that increase future liver remnant (FLR) in order to downstage unresectable CRCLMs [21,22].

Neoadjuvant chemotherapy regimens containing 5-FU, folinic acid, and oxaliplatin and/or irinotecan have been shown to make a significant proportion of previously unresectable CRCLMs amenable to surgery. Furthermore, biologic agents have been commonly used in the treatment of metastatic CRC. Cetuximab and panitumumab are epidermal growth factor receptor (EGFR) inhibitors that are available for KRAS wild-type CRCs, often in a second-line or refractory setting. Bevacizumab is an anti-angiogenic drug that inhibits vascular endothelial growth factor-A (VEGF-A), and is frequently administered as a first-line agent with chemotherapy for metastatic CRC [23].

Optimizing the patient's FLR is a valuable complementary approach to achieving resectability. The FLR is a fundamental determinant of surgical outcome, and the threshold liver volume that must remain after resection is a function of the extent to which the organ has sustained injury, if any. Pre-operative portal vein embolization (PVE) is the main procedure performed to increase the FLR. PVE induces hypertrophy of the FLR by redirecting portal circulation away from the diseased segments [21,22].

A fraction of CRCLMs will remain unresectable despite these measures. Although patients with unresectable disease unfortunately have poorer outcomes, chemotherapy and radiofrequency ablation can be offered as a means of attaining prolonged survival [22].

1.2.2. Histopathological growth patterns

Three different histopathological growth patterns (HGP) have been identified in CRCLMs resected from patients: the 'desmoplastic' HGP, the 'pushing' HGP and the 'replacement' HGP. The characteristic features that determine a CRCLM's growth pattern are present at the interface between the tumour and the adjacent normal liver parenchyma. In the desmoplastic HGP, the cancer cells are enclosed within a desmoplastic stromal ring, physically separating the metastases from the hepatocytes. In the pushing HGP, the cancer cells are in direct contact with the normal liver parenchyma, resulting in the compression of adjacent hepatocytes and vessels, without parenchymal infiltration. In the replacement HGP, the cancer cells replace hepatocytes near the tumour periphery without disrupting adjacent cells or structures within the liver parenchyma (Figure 1) [24,25].

Considering that CRCLMs may present with a combination of growth patterns, current guidelines for scoring the HGPs of liver metastases state that the relative fraction of each growth pattern should be estimated if it represents at least 5% of the length of the tumour-liver interface. A CRCLM can then be categorized as 'predominant desmoplastic HGP', 'predominant pushing HGP' or 'predominant replacement HGP' provided that one growth pattern occupies more than 50% of the tumour margin. This detailed scoring of a CRCLM's HGP is clinically pertinent because "approximately two-thirds of patients present with a mixed growth pattern" and the predominant HGP has prognostic implications [26].

Prior to the initial description of the three CRCLM HGPs by Vermeulen et al. in 2001, it had been reported that fibrotic capsular formation around CRCLMs was an indicator of favourable prognosis. Specifically, in patients who underwent hepatic resection, it was shown that those with liver metastases encapsulated in thick fibrotic tissue had a significantly better five-year survival rate and a lower rate for local recurrence in the remnant liver [27,28]. Severe fibrosis surrounding the metastases is characteristic of the desmoplastic growth pattern, and so it is unsurprising that patients with desmoplastic

HGP CRCLMs were found to have superior overall survival and recurrence-free survival rates compared to those with non-desmoplastic HGP CRCLMs in subsequent studies seeking to examine the growth patterns' prognostic significance [29,30].

Although the biological processes accountable for the differential formation of the three CRCLM HGPs have yet to be elucidated, the mechanisms by which they achieve vascularization have been relatively well-described. The group that originally detailed the histological properties of the distinct HGPs also showed that the replacement growth pattern displayed minimal angiogenesis, unlike the desmoplastic and pushing HGPs [24,31]. It has since been revealed that replacement HGP CRCLMs obtain their blood supply via 'vessel co-option', whereby the cancer cells hijack the mature vasculature of the sinusoidal capillary network within the normal liver parenchyma. In contrast, the desmoplastic HGP CRCLMs are vascularized by VEGF-A-dependent sprouting angiogenesis [32]. This distinguishing feature between replacement and desmoplastic HGP tumours is highly clinically relevant – it has been shown that patients with replacement HGP CRCLMs who received bevacizumab plus chemotherapy (bev-chemo) had a worse pathological response and five-year overall survival than those with desmoplastic HGP CRCLMs receiving the same treatment. Consequently, replacement HGP CRCLMs are resistant to anti-angiogenic therapy through the use of vessel co-option as a means of vascularization [33].

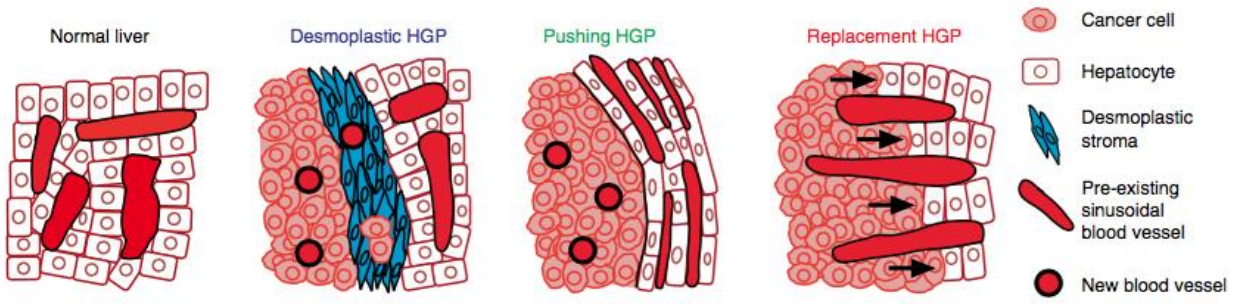

Figure 1: The morphology of the normal liver and the morphology of the tumour–liver interface in liver metastases with a desmoplastic, pushing or replacement HGP

Figure 1(a) from Frentzas S, et al. (2016). Nature Medicine [34].

1.3. **Lysyl oxidases**

1.3.1. Structure and function

The lysyl oxidase (LOX) family of enzymes consists of five secreted copper-dependent amine oxidases which principally participate in the biogenesis and remodelling of the extracellular matrix (ECM) by crosslinking collagen and elastin proteins. Despite being mapped to different chromosomes, the LOX and lysyl oxidase-like 1-4 (LOXL1-4) genes contain several exons with considerable sequence conservation. These shared genomic structures encode a conserved carboxy terminus that encompasses the copper-binding and cytokine receptor-like domains, as well as the lysyl-tyrosylquinone cofactor site required for the lysyl oxidases' enzymatic activity. Conversely, the amino termini show greater variability between the LOX family members, except for the presence of a signal peptide to mark the protein for secretion [34,35]. LOX and LOXL1 are secreted as pro-enzymes, and enzymatic activation is achieved when their N-terminal pro-regions are cleaved by procollagen C-proteinase or mammalian tolloid proteinases. However, prior to proteolytic processing, the pro-regions directly interact with elastic fibres and tropoelastin, which serves to guide the deposition of LOX and LOXL1 to the ECM [36]. LOXL2, LOXL3 and LOXL4 each have four scavenger receptor cysteine-rich (SRCR) domains within their amino termini in place of pro-regions [35]. SRCR domains are ancient, highly-conserved domains that have been found in a multitude of secreted and cell surface proteins, many of which being related to the immune system. Parallels have been drawn between SRCR domains with immunoglobulin and epidermal growth factor-like domains, leading to the idea that they presumably play a role in mediating ligand binding and protein-protein interactions [37]. These putative protein-protein interactions, while not yet well-characterized, constitute part of the premise whereby it is thought that lysyl oxidases are involved in several additional functions, including among others: cell motility, cell adhesion, cell signaling, tumour suppression, and tumour progression [34,35].

1.3.2. Role in forming the pre-metastatic niche

The LOX family members seemingly play a paradoxical role in cancer; both tumour-promoting and tumour-suppressor activities have been reported in studies

investigating the expression and/or function of lysyl oxidases across numerous types of cancer. Nevertheless, it is repeatedly shown that these enzymes are essential mediators of metastasis through their contributions to the formation of the 'pre-metastatic niche'. The pre-metastatic niche refers to the tissue microenvironments of distant organs that have become conducive to colonization by circulating tumour cells. The development of the pre-metastatic niche may occur via diverse mechanisms, though it ultimately necessitates the interaction between secreted tumour-derived factors, host bone marrow-derived cells (BMDC), and stromal elements within the tissue microenvironment [38,39].

Erler et al. were the first to demonstrate the critical role that LOX plays in the formation of metastases from primary breast cancer. MDA231 breast cancer cells were grown in nude mice as orthotopic tumours, after which the associations between hypoxia-induced LOX expression and LOX enzymatic function with metastasis were assessed. Substantial reductions in LOX mRNA and protein levels were seen in tumours that expressed LOX short hairpin RNA, resulting in fewer lung metastases and no liver metastases. Similarly, treatment with either ß-aminoproprionitrile (BAPN), an irreversible inhibitor of LOX family enzymes, or purified LOX antibody resulted in no lung metastases or liver metastases [40]. The mechanism through which LOX promotes metastasis from hypoxic breast cancer was illustrated in a follow-up study by the same group. Hypoxic tumour cells secrete LOX, which colocalized with fibronectin around terminal bronchioles and distal alveoli in the lungs. LOX crosslinked collagen IV in the tissue, facilitating the recruitment and adhesion of CD11b+ BMDCs. These cells produce and secrete matrix metalloproteinase-2 (MMP-2), which catalyzed the cleavage of collagen IV required for BMDC invasion. Furthermore, the breakdown of collagen IV released chemoattractive peptides that recruit circulating tumour cells and additional ECM-remodelling BMDCs to the site. Therefore, LOX was shown to essentially initiate the establishment of the pre-metastatic niche [41].

LOX-mediated collagen crosslinking has also been found to contribute to pre-metastatic niche formation in the context of organ fibrosis, where collagen I is abundant. Cox et al. induced pulmonary fibrosis in immune competent mice and showed that levels of LOX protein were highest in areas of increased collagen I expression. Moreover, following orthotopic implantation of 4T1 breast cancer cells, the increases in the frequency

and size of lung metastases observed in mice with pulmonary fibrosis compared to the controls were significantly mitigated by pre-implant treatment with LOX antibody. An analogous experiment was conducted using mouse models of hepatic fibrosis to investigate whether LOX is equally involved in fibrosis-enhanced metastasis in other organs. Again, metastatic burden was increased in mice with hepatic fibrosis compared to controls, and the administration of LOX antibody prior to the implantation of 4T1 cells considerably reduced the number of liver metastases. Lastly, the cancer cells that had colonized fibrotic tissues displayed improved survival and proliferation, which is thought to be mediated by the LOX-dependent activation of SRC kinase. Collectively, these findings are indicative of LOX's vital role in forming a fibrotic microenvironment that functions as a pre-metastatic niche [42].

Although ECM remodelling via collagen and elastin crosslinking is the primary function of the LOX family members, it is not the only means by which they are capable of forming a pre-metastatic niche. In a retrospective analysis of 344 patients with lymph-node-negative breast cancer who received no adjuvant therapy, strong associations between a hypoxic signature with metastasis and poor survival were exclusively identified in those with estrogen receptor-negative (ER^-) tumours. The association was greatest with bone metastases from primary ER^- breast cancers in particular, which prompted further investigation into a mechanism linking hypoxia to osteotropism [43]. In essence, LOX was shown to disrupt normal bone homeostasis by favouring an osteoclastogenic state, leading to the formation of osteolytic lesions that are known to be more easily colonized by circulating tumour cells. While the mechanism through which LOX activity reduced the number of bone-forming osteoblasts remains to be described, LOX was found to promote the maturation of pre-osteoclasts to bone-resorbing osteoclasts independently of RANKL by inducing the nuclear localization of NFATc1. Thus, LOX-mediated formation of the pre-metastatic niche in bone is achieved indirectly via the stimulation of intracellular processes that alter host cell differentiation [44].

1.3.3. LOXL4 in cancer

LOXL4 was the fifth and last of the lysyl oxidases to be discovered, and its gene structure is most homologous to those of LOXL2 and LOXL3 given its four SRCR

domains. The study in which the sequence of LOXL4 was initially published also revealed that LOXL4 is transcriptionally expressed in various human tissues, including among others: pancreas, skeletal muscle, testis, ovary, lung, and liver [45].

The types of cancer in which the role of LOXL4 has been most heavily researched are those of the head and neck. Several studies have demonstrated that the expression of LOXL4 is substantially upregulated in head and neck squamous cell carcinoma (HNSCC). Specifically, in comparison to either cell cultures or tissue samples of normal squamous epithelium, LOXL4 mRNA and protein were overly expressed in HNSCC cell lines and tumours resected from patients. Furthermore, despite being elevated in primary and metastatic HNSCCs alike, LOXL4 expression significantly correlated with lymph node metastasis and higher tumour stage [46,47]. Consequently, LOXL4 has been identified as a potential diagnostic biomarker and/or therapeutic target in HNSCC. A study that sought to assess the diagnostic and prognostic value of LOXL4 in HNSCC found that 92.7% of 233 primary tumour samples and 97.8% of 45 samples of regional lymph node metastases exhibited LOXL4 protein expression. Contrarily, there was no immunohistochemical evidence of LOXL4 expression in any of the 30 normal oral mucosa samples taken from healthy patients, though positive immunostaining was detectable in intraepithelial neoplasia with moderate- to high-grade dysplasia. Together, these findings indicated that the immunodetection of LOXL4 protein with antibodies like the one used in this study may constitute a highly sensitive and specific diagnostic tool in HNSCC [48]. The therapeutic potential of a new LOXL4 monoclonal antibody (mAb) raised against a similar peptide was examined in a subsequent study. For each of a variety of HNSCC cell lines, severe combined immunodeficiency (SCID) mice were subcutaneously injected with one million cells, either before or after a single intravenous injection of the LOXL4 mAb. In the SCID mice treated with LOXL4 mAb following cancer cell inoculation and visible tumour growth, significant regression was observed for 12 of the 15 HNSCC cell lines. Meanwhile, in those pre-immunized with LOXL4 mAb, tumour growth was greatly delayed relative to the untreated SCID control mice. These results strengthen the candidature of LOXL4 as a promising target in the treatment of HNSCC [49]. Lastly, a feasibility study was conducted to determine whether a dendritic cell-based tumour vaccine could be developed with LOXL4 as the target antigen. Immature dendritic cells were harvested from healthy

individuals, transfected with LOXL4 mRNA, and cultured with a mixture of growth factors and pro-inflammatory cytokines to induce maturation. The LOXL4-mRNA-transfected dendritic cells were shown to induce LOXL4-specific cytotoxic T lymphocytes *in vitro*, which showed enhanced secretion of interferon gamma when stimulated with LOXL4-positive T cells [50].

As is the case with the other LOX family members, both pro- and anti-tumour roles have been attributed to LOXL4 across various types of cancer. For example, there is evidence suggesting that LOXL4 may exhibit tumour-suppressor activity in bladder cancer and hepatocellular carcinoma (HCC). The expression of LOXL4 was surveyed in seven bladder cancer cell lines and one immortalized uroepithelial cell, of which five had gene silencing. The administration of a demethylating agent reversed the loss of expression, revealing hypermethylation to be the mechanism responsible. Moreover, methylation of the LOXL4 gene was seen in 40% of 63 primary bladder tumours collected from patients, with a comparable proportion of these tumours having reduced levels of LOXL4 expression. Additional investigations showed that LOXL4 can act as a direct inhibitor of the Ras/ERK signalling pathway, resulting in the impaired colony formation of bladder cancer cells [51]. Whereas LOXL4 had the ability to negatively regulate cell proliferation in bladder cancer, its activity as a tumour suppressor in HCC was found to potentially involve TGF-ß1 signalling. The overexpression of LOXL4, whose transcription is itself induced by TGF-ß1 through Smad proteins and AP-1 transcription factors, decreased the invasiveness of HCC cells *in vitro* and antagonized the expression of other TGF-ß1-induced factors known to promote motility, invasion, and metastasis [52,53]. Furthermore, in a cohort of 298 HCC patients, low expression levels of LOXL4 was significantly associated with worse overall survival and earlier time to recurrence following curative resection [54]. These findings collectively point to LOXL4 having a protective effect against some types of cancer.

Conversely, there is evidence of LOXL4 having a pro-metastatic role in several types of cancer, such as gastric cancer and ovarian cancer. LOXL4 expression was elevated in gastric carcinomas resected from patients compared to the adjacent normal tissues, and it was significantly associated with tumour size, depth of tumour invasion, lymph node metastasis, TNM stage, and overall survival. Increasing the expression of LOXL4 in gastric

cancer cell lines also led to enhanced proliferation, migration, and invasion *in vitro*. This augmented tumour cell aggressiveness was thought to be a consequence of FAK/Src/ERK pathway activation because the phosphorylation of these kinases corresponded to higher levels of LOXL4 [55]. The pro-metastatic role of LOXL4 in ovarian cancer that was described by Sebban et al. is rather unique since it concerns alternatively spliced isoforms. Two splice variants of LOXL4 mRNA were identified in the primary tumours and/or effusions from patients with ovarian cancer, breast cancer, and malignant mesothelioma [56]. Inducing the expression of LOXL4 splice variants in ovarian carcinoma ES-2 cells resulted in increased invasion, MMP-2 activity, and mesenchymal marker expression. Similarly, the injection of splice variant-expressing ES-2 cells in SCID mice produced metastases in numerous sites that were not seen in the control animals, and upregulated the transcription of oncogenic microRNAs. These findings are especially intriguing considering that neither the translation of the LOXL4 splice variant mRNAs nor the enzymatic activity of LOXL4 were required to generate the pro-metastatic effects observed in this study [57].

1.4. **Extracellular vesicles**

1.4.1. Structure and function

The role of extracellular vesicles (EV) as mediators of intercellular communication is a relatively recent and emerging field of research where much has yet to be discovered. EVs consist of a lipid bilayer embedded with transmembrane proteins that envelops cargo containing cytosolic proteins, lipids, DNA, and RNA. EVs are typically subcategorized into exosomes and microvesicles based on their size and mechanism of release. Exosomes range approximately from 40-120 nm in diameter and are released via mutlivesicular endosome fusion with the plasma membrane, whereas microvesicles can measure greater than 1000 nm in diameter and bud directly from the plasma membrane [58,59]. Apart from merely acknowledging that these different terms exist in the literature, the types of EVs will not be distinguished hereafter.

The list of functions that have been attributed to EVs is continuously expanding and includes activities in both normal and pathologic processes. The studies investigating these functions span a multitude of disciplines, such as immunology, neurology, and oncology. For example, EVs have been shown to participate in antigen presentation, immune response regulation, signalling pathway activation, neuronal growth and survival, and in the promotion of metastasis. The diverse utility that EVs possess is thought to be due in part to the wide range of molecules that they can deliver to target cells. Many cell types are known to secrete EVs, which explains the intrinsic variety of lipids and proteins that make up their outer structure and cargo. Furthermore, EVs carry an assortment of RNA molecules: mRNAs, microRNAs, small interfering RNAs, and other small non-coding RNAs. Together, these EV-packaged macromolecules can substantially regulate the behaviour of the cells to which they are transmitted [58,59].

1.4.2. EVs in cancer

There is a growing body of evidence suggesting that EVs play pro-tumourigenic and pro-metastatic roles in cancer progression. Although their physiological activities may be supportive of disease in this context, EVs have also become an attractive target for new diagnostic tests and treatments [60].

Two mechanisms through which EVs are speculated to promote tumourigenesis are the suppression of anti-tumour immunity and the stimulation of angiogenesis. EVs can facilitate immune evasion in cancer by inhibiting the function of natural killer cells and cytotoxic T lymphocytes, while simultaneously stimulating myeloid-derived suppressor cells and regulatory T cells. The result of this EV-induced leukocyte regulation would be the establishment of a tolerant immune environment that is conducive to tumour growth and development. However, it should be noted that EVs can also be involved in activating immune responses against cancer cells; their role in the immune system is not necessarily unidirectional [61,62]. The promotion of angiogenesis is another hallmark of cancer where EVs are implicated. Tumour cells secrete EVs directed towards endothelial cells and pericytes that may contain growth factors, cytokines, and functional RNA molecules. Among the effects of these EV-mediated interactions are increased endothelial cell proliferation, migration, and tube formation, as well as pericyte activation [63,64].

In addition to supporting the growth and survival of primary tumours, EVs promote metastasis by enhancing cancer cell invasion and helping to form the pre-metastatic niche. Non-neoplastic cells within the tumour microenvironment can secrete EVs that increase cancer cell motility, invasiveness, and dissemination through the activation of signalling pathways. EVs may also induce epithelial-mesenchymal transition in recipient tumour cells, which is known to enable metastasis [65]. Besides conferring cancer cells with an aggressive phenotype, EVs can modify vascular endothelial and parenchymal cells. Select microRNAs transmitted by tumour cell-derived EVs can disrupt blood vessel integrity by weakening the intercellular junctions between endothelial cells, ultimately leading to augmented vascular permeability. Furthermore, once the cancer cells have extravasated through leaky vessels, EVs contribute to the formation of the pre-metastatic niche by stimulating ECM remodelling and the recruitment of stromal cells in distant organs [65,66].

The potential applications of liquid biopsies in the diagnosis and monitoring of cancer have made EVs an enticing biomarker in oncology [67]. EVs have been isolated from a variety of bodily fluids, including: blood, saliva, urine, cerebrospinal fluid, bile, semen, breast milk, and amniotic fluid [58]. Several studies have identified circulating DNA and RNA molecules carried within EVs that were significantly enriched in cancer patients compared to healthy individuals [68-70]. While this field is in its early stages, it is

not unreasonable to presume that these cancer-associated markers might eventually become clinically valuable.

Chapter 2: Body of the Thesis

Introduction

Rationale

Having established that liver metastases from primary colorectal cancer is a major cause of cancer-related death, it is evident that optimizing patients' chemotherapeutic regimens to achieve resectability and improve overall survival, among other outcomes, is a clinically important matter. The evidence suggesting that a CRCLM's predominant growth pattern has prognostic implications points to the HGP possibly serving as a predictive biomarker of response to anti-angiogenic therapy, when no such biomarker has been validated to date. However, the current guidelines for HGP scoring state that growth patterns are to be evaluated by a pathologist via light microscopic imaging of resected liver metastatic tissue, implying that preoperative treatment precedes HGP assessment. Therefore, surrogate molecular markers for the HGPs that can be appraised prior to surgery would be helpful to inform clinical decision-making about whether a patient with CRCLM may benefit from anti-angiogenic treatment, in addition to neoadjuvant chemotherapy.

Furthermore, the pathophysiological processes that drive the distinct growth patterns with which CRCLMs may present remain largely unknown. Investigating the differential gene expression between replacement and desmoplastic HGP CRCLMs may shed light on the underlying molecular mechanisms responsible for this heterogeneity.

Objectives

It is hypothesized that there are unique cellular and molecular processes promoting the formation of replacement HGP CRCLMs, and that the identification of genes and pathways that are differentially regulated to generate the replacement HGP phenotype may uncover potential diagnostic biomarkers and targets for anti-metastatic therapy. In order to test this hypothesis, we sought to characterize the global gene expression profile of replacement and desmoplastic HGP CRCLMs resected from chemonaïve patients, with the following objectives. Objective 1: Analyze RNA sequencing (RNA-Seq) data to identify differentially expressed genes (DEG) that are significantly upregulated in the replacement HGP CRCLMs compared to the desmoplastic HGP CRCLMs and adjacent normal liver tissues, from which a replacement HGP metastasis gene signature will be generated. Objective 2: Study the immunohistochemical expression of select DEGs from this gene expression signature in chemonaïve replacement and desmoplastic HGP lesions. Objective 3: Isolate EVs from the plasma of CRCLM patients and assess whether their contents include the gene products of select DEGs from the replacement HGP metastasis gene signature.

Methodology

2.2.1. Human samples

Blood and CRCLM specimens were obtained through the MUHC-Research Institute Liver Disease Biobank from patients who underwent surgical resection at the Royal Victoria Hospital in Montreal. Informed consent was obtained from all patients, and ethical approval was granted by the McGill University Health Centre (MUHC) Research Ethics Board. The patients from whom these specimens were collected were either chemonaïve (no preoperative therapy) or treated preoperatively with a combination of bevacizumab and chemotherapy (Table 1 in Supplementary Tables).

2.2.2. RNA sequencing

Total RNA was extracted from 18 chemonaïve CRCLM snap-frozen lesions (9 desmoplastic HGP, 6 replacement HGP, and 3 'mixed' HGP), and from paired adjacent normal liver specimens. RNA-Seq was performed by the Samsung Genome Institute, through collaborations with Dr. Woong-Yang Park. The library construction was done using the TruSeq RNA sample preparation v2 kit (Illumina). The quality and quantity of the library were measured by Bioanalyzer and Qubit. Sequencing was carried out using the 100-bp paired-end mode of the TruSeq Rapid PE Cluster kit and TruSeq Rapid SBS kit (Illumina) on the HiSeq 2500 sequencing platform (Illumina).

2.2.3. Gene expression signature

A gene signature was manually generated from the RNA-Seq data in order to identify DEGs whose expression levels were upregulated in the replacement HGP CRCLMs relative to both the desmoplastic HGP CRCLMs and the normal liver specimens. The DEGs that were included in the gene expression signature meet the following three conditions. I) The mean of normalized counts in the replacement HGP specimens is greater than 100. II) The fold change in the replacement HGP lesions relative to the desmoplastic HGP lesions is significantly greater than 2 ($p<0.05$). III) The fold change in the replacement HGP lesions relative to the adjacent normal liver specimens is significantly greater than 2 ($p<0.05$).

2.2.4. H&E staining

Formalin-fixed paraffin-embedded (FFPE) tissue blocks were cut into sections 4 μm in thickness using a microtome. Sections were deparaffinized, rehydrated, stained and dehydrated according to the H&E staining protocol optimized by the MUHC Ocular Pathology Laboratory, directed by Dr. Miguel Burnier (Figure 12 in Supplementary Methods). Slides were scanned at 40X magnification using the Aperio AT Turbo system (total magnification of 400X) and viewed using the Aperio ImageScope software program.

2.2.5. Immunohistochemistry

FFPE tissue blocks were cut into sections 4 μm in thickness, which were deparaffinized and rehydrated according to standard protocols. Heat-induced epitope retrieval was performed at pH 6.0 in a steamer. Sections were incubated with peroxidase block (Dako) for 20 minutes, followed by incubation in blocking buffer (5% goat serum in 1% PBS-T) for 1 hour at room temperature. Sections were then incubated overnight at 4°C with primary antibody diluted in blocking buffer. Primary antibodies were detected with the EnVision+ System-HRP (Dako, K4007) for DAB staining, and counterstained with hematoxylin prior to mounting under cover glasses (Figure 13 in Supplementary Methods). Slides were scanned at 40X magnification using the Aperio AT Turbo system (total magnification of 400X) and images were viewed using the Aperio ImageScope software for scoring analysis and signal assessment.

The primary antibodies that were used are the following: anti-CXCL6 (Signalway Antibody, 43727; dilution 1:1000), anti-EpCAM (Abcam, ab71916; dilution 1:200), anti-Hep Par-1 (Santa Cruz Biotech, sc-58693; dilution 1:500), anti-LOXL4 (Sigma-Aldrich, HPA037609; dilution 1:200), anti-TNC (Invitrogen, MA1-26779; dilution 1:4000), and anti-VIM (Abcam, ab16700; dilution 1:200).

2.2.6. Immunofluorescence

FFPE tissue blocks were cut into sections 4 μm in thickness, which were deparaffinized and rehydrated according to standard protocols. Heat-induced epitope retrieval was performed at pH 6.0 in a steamer. Sections were incubated with peroxidase block (Dako) for 20 minutes, followed by incubation in blocking buffer (5% goat serum in

1% PBS-T) for 1 hour at room temperature. Sections were then incubated overnight at 4°C with primary antibody diluted in blocking buffer. Following the removal of primary antibody, sections were washed and incubated with secondary antibody for 2 hours at room temperature. Sections were washed once more after the secondary antibody was removed, and subsequently incubated with a 1:1000 dilution of DAPI (Thermo Fisher Scientific, D1306) in PBS for 10 minutes at room temperature. Prior to mounting under cover glasses, 1-2 drops of ProLong® Gold Antifade Mountant (Thermo Fisher Scientific, P36934) were added to each section (Figure 14 in Supplementary Methods). Slides were visualized at the RI-MUHC Molecular Imaging Platform using a Zeiss LSM780 confocal microscope.

The primary antibodies that were used are the following: anti-Pan-Cytokeratin (Dako, M3515; dilution 1:200) and anti-VIM (Abcam, ab16700; dilution 1:200). The secondary antibodies that were used are the following: Alexa Fluor® 488 conjugated goat anti-mouse IgG/IgM (Invitrogen, A-10680; dilution 1:1000) and Alexa Fluor® 568 conjugated donkey anti-rabbit IgG (Invitrogen, A10042; dilution 1:1000).

2.2.7. Statistical analysis

Statistical analysis was performed with a two-tailed Fisher's exact test or a two-tailed Student's t-test using Microsoft Excel. *P* values less than 0.05 were considered to be statistically significant.

2.2.8. Extracellular vesicle isolation

EVs were isolated from 3 mL aliquots of fresh frozen plasma by differential centrifugation. Plasma samples were centrifuged at 2,000*g* for 10 minutes at 4°C, and the supernatants were transferred to polyallomer centrifuge tubes (Beckman Coulter, 361623). The supernatants were diluted with cold PBS (Thermo Fisher Scientific, 10010023) to a final volume of 9 mL, then centrifuged at 10,000*g* for 20 minutes at 4°C using a Type 80 Ti fixed angle rotor. The supernatants were transferred to new polyallomer centrifuge tubes, and centrifuged at 100,000*g* for 90 minutes at 4° using a Type 80 Ti fixed angle rotor. The supernatants were discarded, and the pelleted EVs were resuspended in lysis buffer for further experimentation.

2.2.9. Protein detection

Lysed EVs were separated on 10% SDS-PAGE gels at 50V for 15 minutes, then 120V for 60 minutes. Proteins were transferred to nitrocellulose membranes at 320mA for 80 minutes. The membranes were blocked using blocking buffer (5% skimmed milk powder in TBS-T) and blotted with antibodies against LOXL4 (Sigma-Aldrich, HPA037609; dilution 1:250), TAPA-1 (Abcam, ab79559; dilution 1:500), and TSG101 (BD Biosciences, 612696; dilution 1:500). The membranes were then incubated with HRP-conjugated secondary antibodies (Cell Signalling Technology, 7076; dilution 1:20,000) for 60 minutes, followed by visualization using the Amersham Western Blotting Detection Kit and digital image acquisition using the ImageQuant LAS 400 camera system.

Results

2.3.1. Gene expression signature for replacement HGP CRCLMs

Initial analysis of the RNA-Seq data revealed that 525 genes were significantly differentially expressed ($p<0.05$) between the chemonaïve replacement and desmoplastic HGP CRCLMs whose RNA had been sequenced. Among them, 53 DEGs met the three aforementioned conditions for inclusion in the replacement HGP CRCLM gene expression signature (Table 2 in Supplementary Tables).

2.3.2. LOXL4 expression in chemonaïve replacement and desmoplastic HGP CRCLMs

LOXL4 was identified as a DEG whose transcription is significantly upregulated in replacement HGP CRCLMs compared to the desmoplastic HGP CRCLMs (fold change of 5.6) and adjacent normal liver tissues (fold change of 6.2). To determine whether these increases in LOXL4 mRNA levels translated to comparable differences in protein expression, LOXL4 protein was detected in 10 chemonaïve replacement HGP and 10 chemonaïve desmoplastic HGP CRCLMs by IHC.

In the replacement HGP CRCLMs, positive staining was mostly confined to cells located at the tumour-liver interface and in some areas of inflammation, though a small number of LOXL4-expressing cells were also scattered throughout the liver parenchyma (Figure 2A and Figure 2B). The main difference in the desmoplastic HGP CRCLMs with regards to LOXL4 protein expression was one of quantity rather than location. Although positively-stained cells were identified at the borders of desmoplastic rings, areas of inflammation, and within the liver parenchyma, they were visibly less numerous compared to what was observed in the replacement HGP CRCLMs (Figure 2C and Figure 2D). Furthermore, the regions in which the most LOXL4-expressing cells were located in select predominant desmoplastic HGP CRCLMs were the areas of budding replacement HGP growth (Figure 3). These LOXL4-expressing cells in all 20 chemonaïve specimens were neither tumour cells nor hepatocytes.

Digital image analysis supported these observations, revealing that the levels of LOXL4 protein were significantly elevated in the chemonaïve replacement HGP CRCLMs at the interface (fold change of 7.1, *P* value of 0.005) and in the zones of inflammation

(fold change of 2.8, *P* value of 0.004) compared to the desmoplastic HGP CRCLMs (Figure 4).

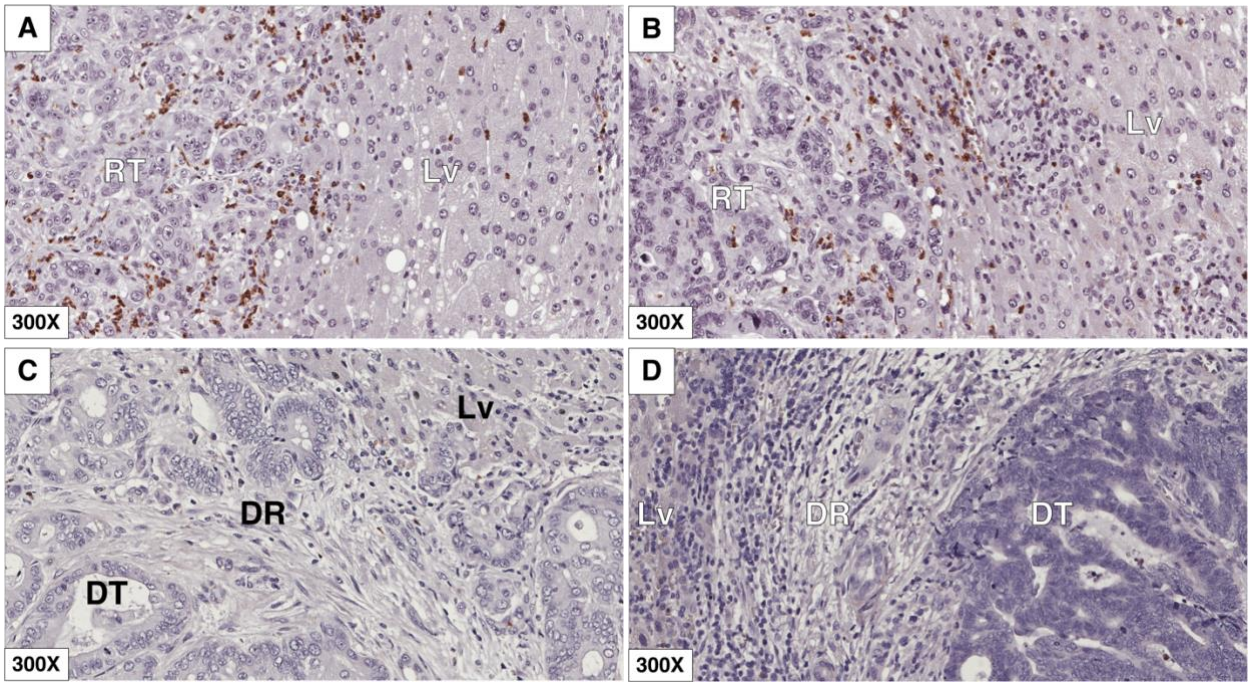

Figure 2: LOXL4 staining in chemonaïve replacement (A,B) and desmoplastic (C,D) HGP CRCLMs. RT, replacement HGP tumour; Lv, liver parenchyma; DT, desmoplastic HGP tumour; DR, desmoplastic ring.

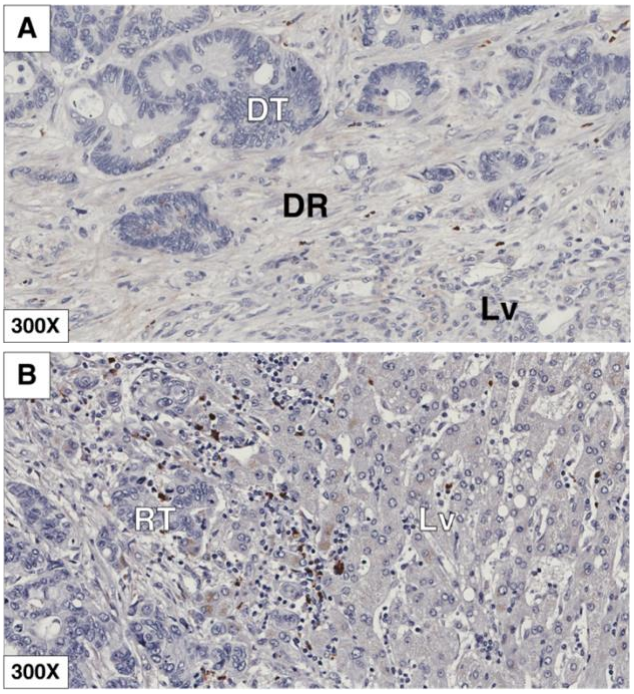

Figure 3: LOXL4 staining in a desmoplastic HGP CRCLM (A) with budding replacement HGP growth (B). DT, desmoplastic HGP tumour; DR, desmoplastic ring; Lv, liver parenchyma; RT, replacement HGP tumour.

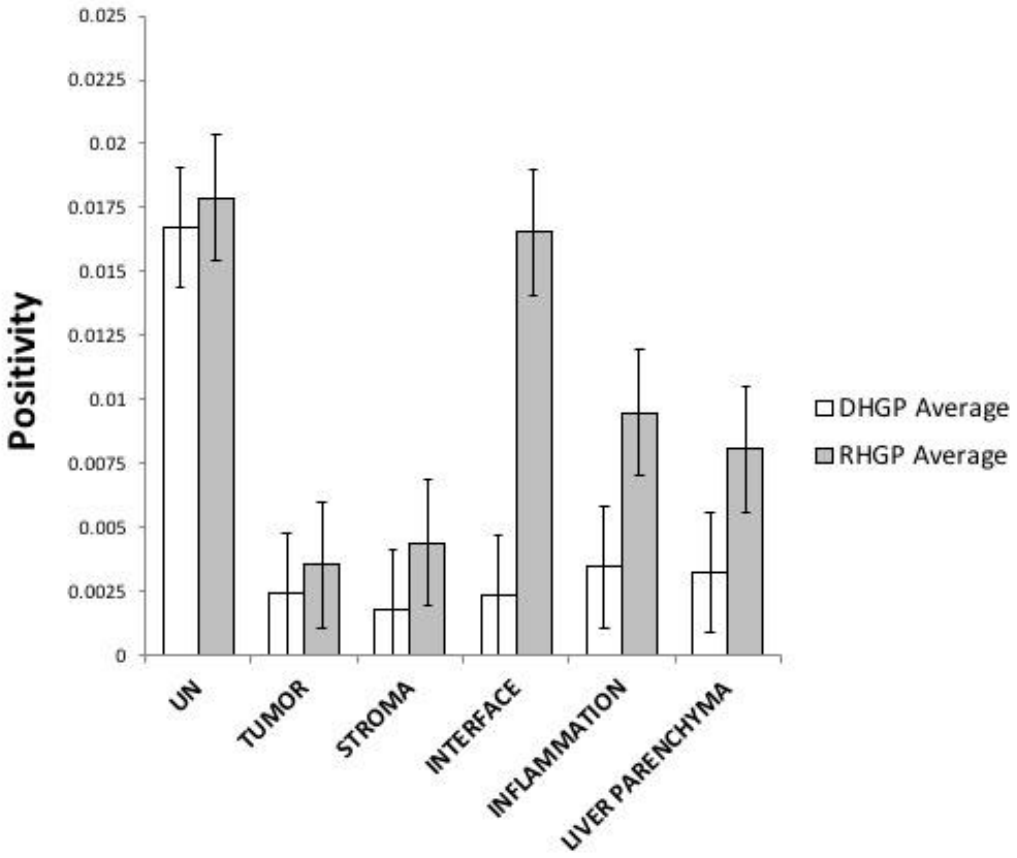

Figure 4: Digital image analysis of LOXL4 immunohistochemical staining in chemonaïve replacement and desmoplastic HGP CRCLMs stratified by areas of interest. UN, usual necrosis; DHGP, desmoplastic HGP; RHGP, replacement HGP.

2.3.3. LOXL4 expression in bev-chemo replacement and desmoplastic HGP CRCLMs

The expression of LOXL4 protein was also immunohistochemically detected in five replacement HGP and five desmoplastic HGP CRCLMs that had been treated with bev-chemo.

The staining pattern that was seen in the chemonaïve replacement HGP CRCLMs was maintained, with all but one of the treated replacement HGP metastases having LOXL4-expressing non-neoplastic cells present at the tumour-liver interface. Furthermore, there were many positively-stained cells in areas of necrosis within the tumour in all five replacement HGP samples.

Three out of five treated desmoplastic HGP CRCLMs had LOXL4-positive cells at the exterior border of the desmoplastic ring, though they were noticeably fewer than those at the replacement HGP interface. Unlike the treated replacement HGP CRCLMs, there was a relative absence of positively-stained cells in the areas of tumour necrosis in the desmoplastic HGP metastases. In fact, the necrotic areas within these tumours were generally acellular.

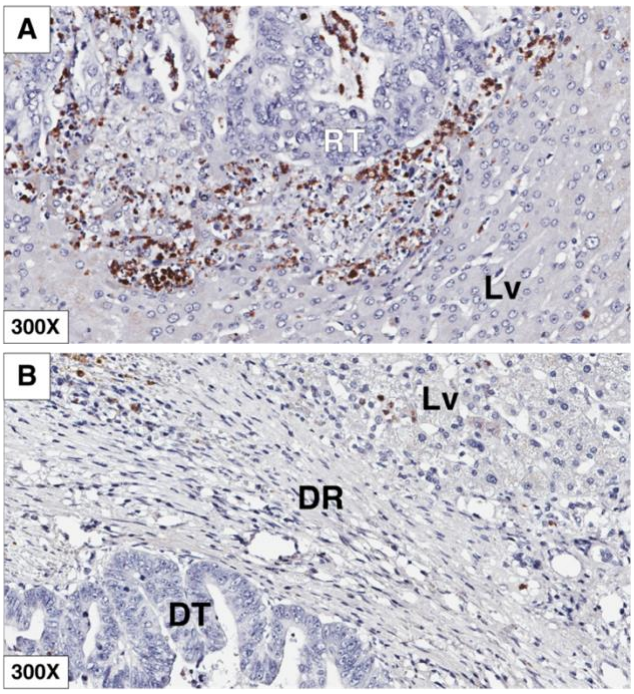

Figure 5: LOXL4 staining in replacement (A) and desmoplastic (B) HGP CRCLMs treated with bev-chemo. RT, replacement HGP tumour; Lv, liver parenchyma; DT, desmoplastic HGP tumour; DR, desmoplastic ring.

2.3.4. CXCL6 expression in chemonaïve replacement and desmoplastic HGP CRCLMs

CXCL6 was identified as a DEG whose transcription is significantly upregulated in replacement HGP CRCLMs compared to the desmoplastic HGP CRCLMs (fold change of 8.8) and adjacent normal liver tissues (fold change of 5.5). To determine whether these increases in CXCL6 mRNA levels translated to comparable differences in protein expression, CXCL6 protein was detected in 10 chemonaïve replacement HGP and 10 chemonaïve desmoplastic HGP CRCLMs by IHC.

The strongest staining intensity was observed in tumour cells and cholangiocytes. The hepatocytes also appeared to be weakly positive in most samples, though significantly less so compared to the tumour tissue and bile ducts. Meanwhile, there was no staining in the stroma within the tumour or liver parenchyma, nor in the areas of inflammation. There were no evident HGP-related distinctions in the immunostaining patterns for CXCL6.

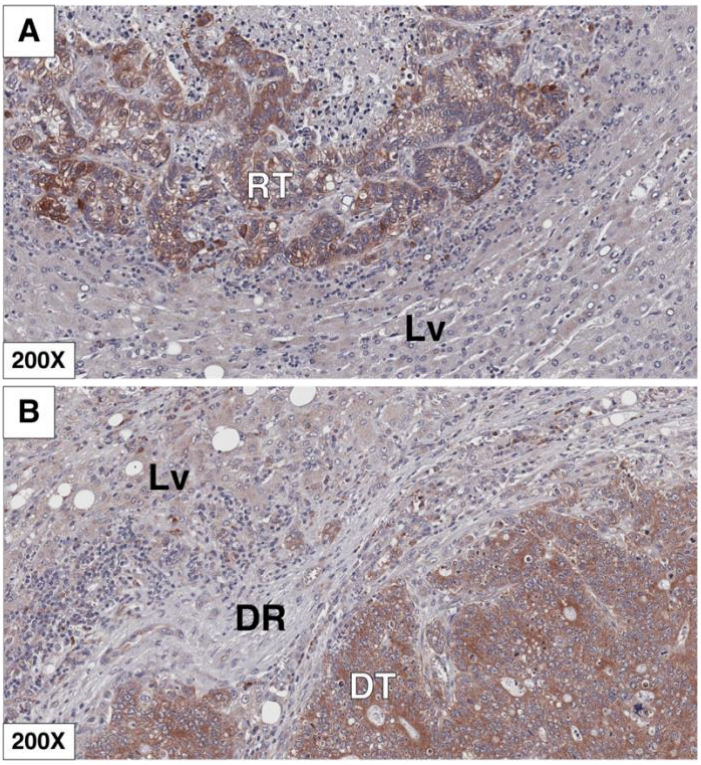

Figure 6: CXCL6 staining in chemonaïve replacement (A) and desmoplastic (B) HGP CRCLMs. RT, replacement HGP tumour; Lv, liver parenchyma; DR, desmoplastic ring; DT, desmoplastic HGP tumour.

2.3.5. TNC expression in chemonaïve replacement and desmoplastic HGP CRCLMs

TNC was identified as a DEG whose transcription is significantly upregulated in replacement HGP CRCLMs compared to the desmoplastic HGP CRCLMs (fold change of 3.8) and adjacent normal liver tissues (fold change of 34.1). To determine whether these increases in TNC mRNA levels translated to comparable differences in protein expression, TNC protein was detected in five chemonaïve replacement HGP and five chemonaïve desmoplastic HGP CRCLMs by IHC.

Positive staining was most intense and abundant in the tumour stroma surrounding the cancer cells in all of the samples, though the tumour cells themselves were negative. Similarly, the hepatocytes in the adjacent normal liver were negative as well. The only regions within the liver parenchyma that showed positive staining for TNC were select areas of inflammation, particularly those within close proximity of portal triads. Overall, there were no apparent differences between the expression patterns of TNC protein between the replacement and desmoplastic HGP specimens.

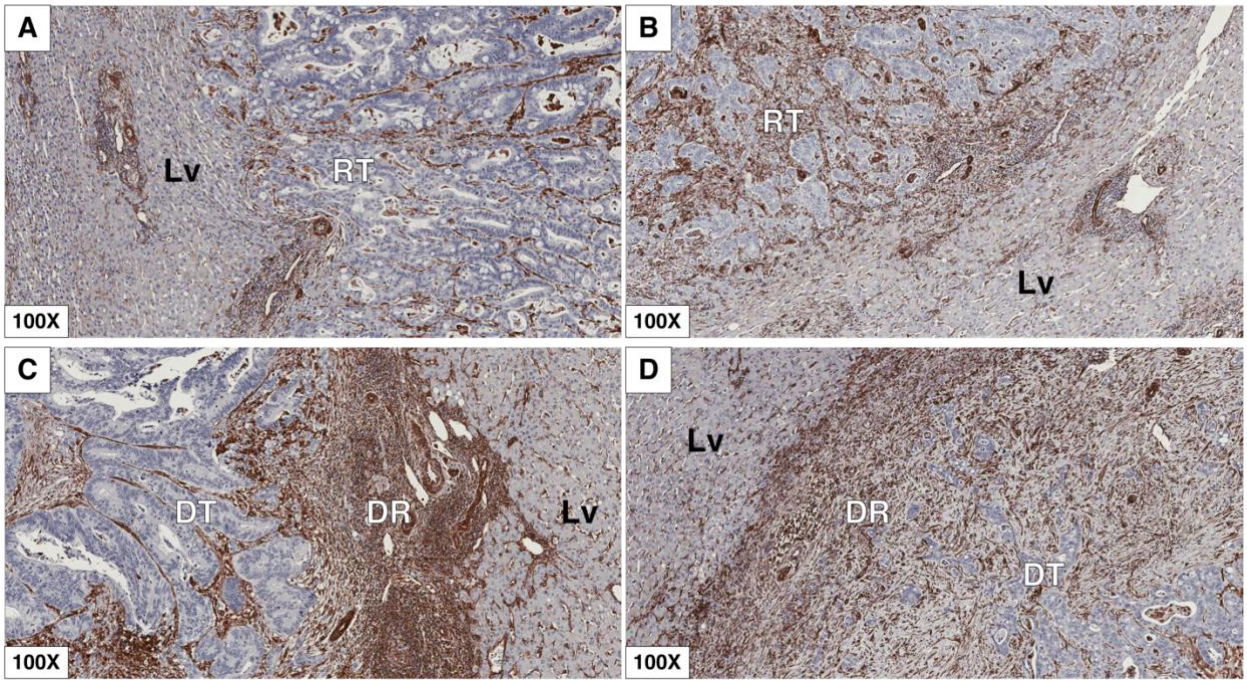

Figure 7: TNC staining in chemonaïve replacement (A,B) and desmoplastic (C,D) HGP CRCLMs. Lv, liver parenchyma; RT, replacement HGP tumour; DT, desmoplastic HGP tumour; DR, desmoplastic ring.

2.3.6. Hep Par-1 expression in chemonaïve replacement and desmoplastic HGP CRCLMs

The expression of Hep Par-1 protein was detected in 10 chemonaïve replacement HGP and 10 chemonaïve desmoplastic HGP CRCLMs by IHC. Positive staining was specific to hepatocytes, though the intensity, both within and between samples, was not always uniform. There was a relative absence of Hep Par-1-positive cells within the central tumour of desmoplastic HGP CRCLMs, as the hepatocytes were largely kept outside the desmoplastic ring. However, positively- stained cells were identified in several replacement HGP CRCLMs. These Hep Par-1-expressing cells were mostly located at the periphery of the metastases, though some were found to have infiltrated more than 1 cm beyond the tumour-liver interface.

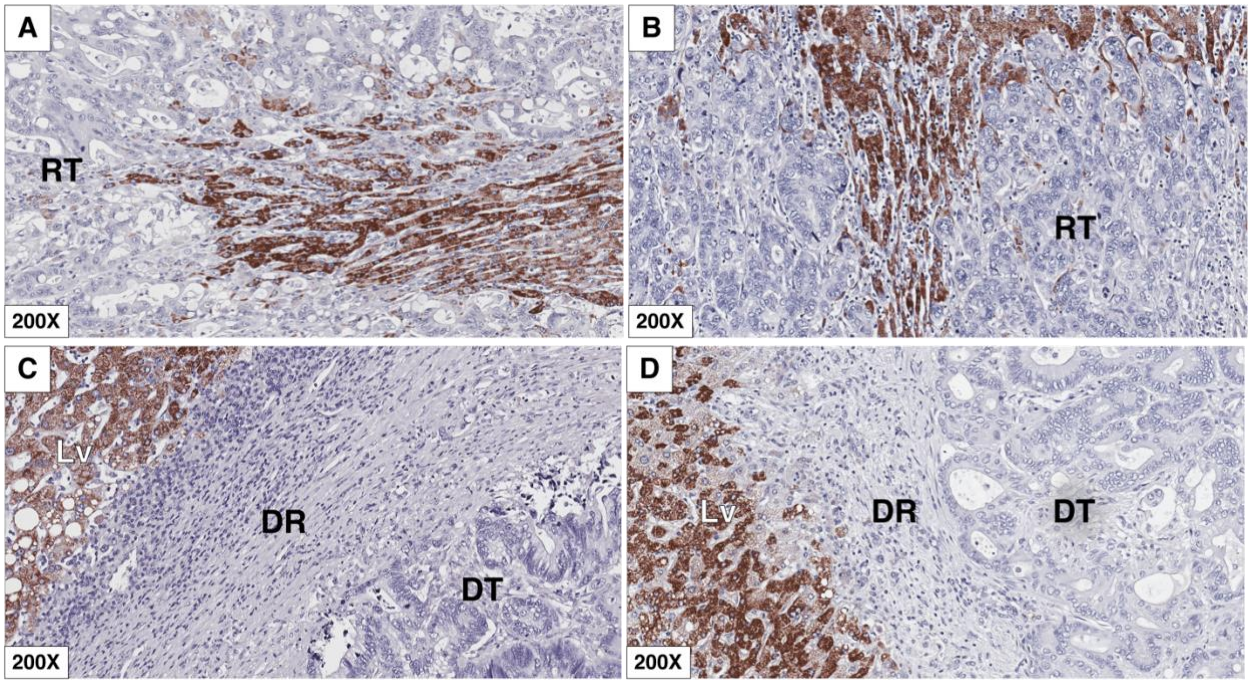

Figure 8: Hep Par-1 staining in chemonaïve replacement (A,B) and desmoplastic (C,D) HGP CRCLMs. RT, replacement HGP tumour; Lv, liver parenchyma; DR, desmoplastic ring; DT, desmoplastic HGP tumour.

2.3.7. EpCAM expression in chemonaïve CRCLMs and benign liver pathologies

The expression of EpCAM protein was immunohistochemically detected in two chemonaïve replacement HGP and two chemonaïve desmoplastic HGP CRCLMs, as well as in two specimens of benign liver disease. Specifically, these benign pathologies consisted of a liver cyst and a hemangioma. Tumour cells and cholangiocytes stained strongly for EpCAM, whereas hepatocytes and stroma were devoid of staining. Positive EpCAM immunoreactivity was therefore abundant in the replacement and desmoplastic HGP CRCLMs, while being minimally detectable in the cyst and hemangioma specimens where it was exclusively confined to the bile ducts.

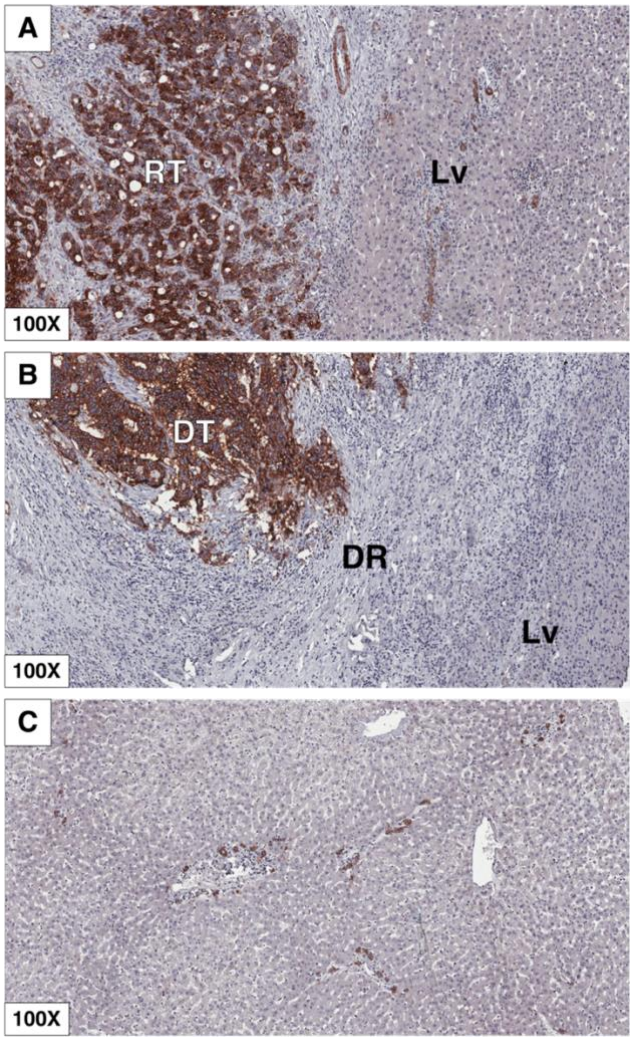

Figure 9: EpCAM staining in chemonaïve CRCLMs (A,B) and benign liver pathologies (C). RT, replacement HGP tumour; Lv, liver parenchyma; DT, desmoplastic HGP tumour; DR, desmoplastic ring.

2.3.8. VIM expression in chemonaïve replacement and desmoplastic HGP CRCLMs

The expression of VIM protein was detected in 10 chemonaïve replacement HGP and 10 chemonaïve desmoplastic HGP CRCLMs by IHC. In all samples, positive staining was localized to the tumour stroma, portal triads, areas of inflammation, and Kupffer cells. The desmoplastic rings were also positive for VIM protein in the desmoplastic HGP metastases. The tumour cells and hepatocytes were generally negative, though some weakly positive staining in these cells was seen in select samples.

The simultaneous expression of VIM and Pan-Cytokeratin proteins was also detected in two chemonaïve replacement HGP and two chemonaïve desmoplastic HGP CRCLMs by immunofluorescence (IF). The staining pattern for VIM in IF was consistent with that in IHC, where the stroma was strongly positive. The tumour cells uniformly expressed Pan-Cytokeratin, though there was a lack of co-localization with VIM in the few samples that were stained according to the IF protocol (data not shown).

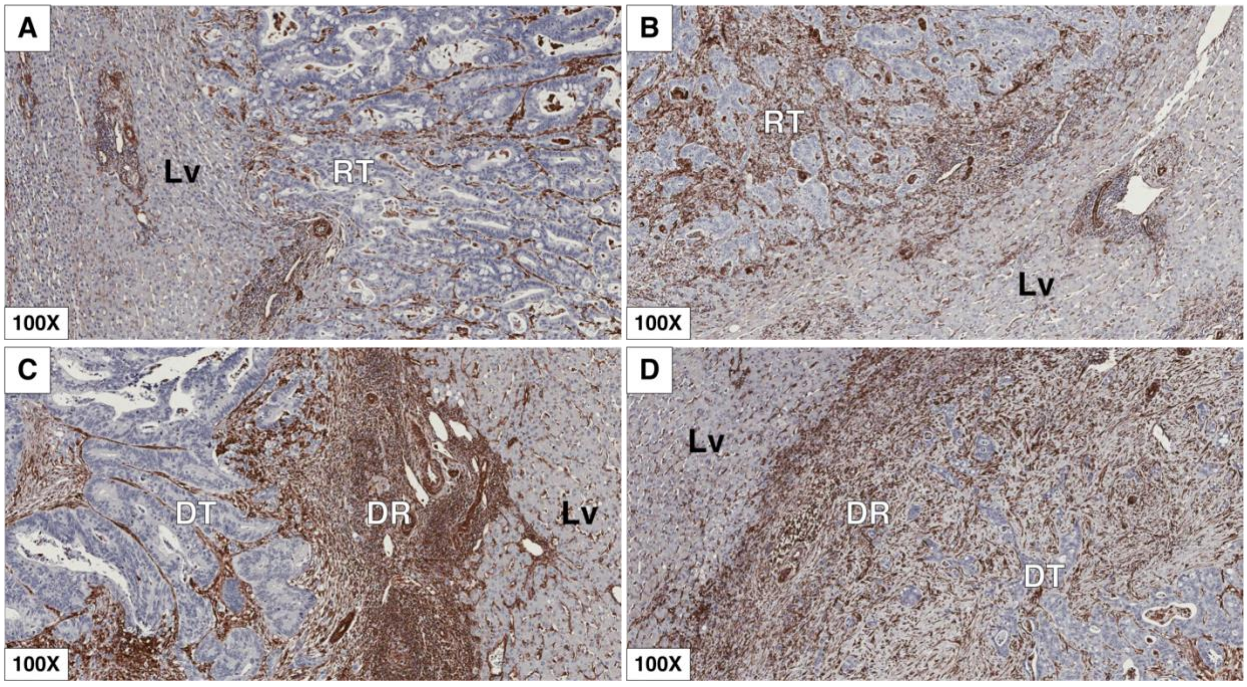

Figure 10: VIM staining in chemonaïve replacement (A,B) and desmoplastic (C,D) HGP CRCLMs. Lv, liver parenchyma; RT, replacement HGP tumour; DT, desmoplastic HGP tumour; DR, desmoplastic ring.

2.3.9. Isolation of EVs from patient plasma and detection of EV-transported proteins

EVs were isolated from the plasma of six patients by differential centrifugation. These patients consisted of two with replacement HGP CRCLMs, two with desmoplastic HGP CRCLMs, and two with benign liver pathologies. The isolation of EVs was confirmed by Nanoparticle Tracking Analysis (NTA), which revealed a significant increase in the concentration of particles whose diameters measured less than 1000 nm (data not shown).

The pelleted EVs were then resuspended in lysis buffer for the subsequent detection of CD81/TAPA-1, TSG101, and LOXL4 proteins by Western blot. Bands for these three proteins were present for all six samples. The most notable observations derived from the samples' banding patterns were that TSG101 appeared to be most abundant in the pair of benign disease cases, and that multiple bands were seen in the detection of LOXL4.

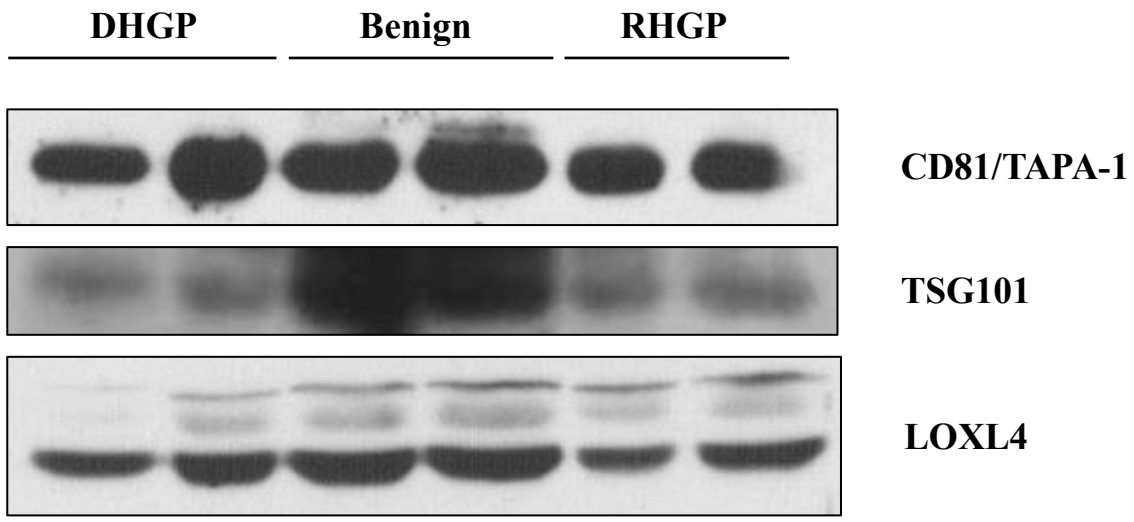

Figure 11: Western blot analysis of CD81/TAPA-1, TSG101, and LOXL4 from EVs isolated from the plasma of patients with CRCLM or benign liver disease. DHGP, desmoplastic HGP; RHGP, replacement HGP.

Discussion

Colorectal cancer is among the most common types of cancer in North America, and is a leading cause of cancer-related death. Colorectal cancer liver metastasis is responsible for the majority of these deaths, though survival rates have been improving due to advances in the surgical and chemotherapeutic management of patients with metastatic disease. Angiogenesis inhibitors, like bevacizumab, constitute one of these advances, and are used in the treatment of metastatic CRC as an adjunct to neoaduvant chemotherapy. However, variability exists in CRCLM response to bev-chemo. Histopathological growth patterns in liver metastases have emerged as potential predictive biomarkers for susceptibility or resistance to anti-angiogenic therapy. CRCLMs that present with the replacement HGP have been shown not to benefit from neoadjuvant bevacizumab, though surrogate biomarkers for these tumours have yet to be identified.

In this study, we have sequenced total RNA extracted from chemonaïve CRCLMs stratified by growth pattern for the first time, and have subsequently identified differentially expressed genes whose transcription is significantly upregulated in replacement HGP CRCLMs compared to desmoplastic HGP CRCLMs and normal liver parenchyma. We also compared the protein expression levels of select DEGs between chemonaïve replacement and desmoplastic HGP CRCLMs by immunohistochemistry. Our data showed that, in addition to there being increased levels of LOXL4 mRNA in replacement HGP CRCLMs, LOXL4 protein was elevated at the tumour-liver interface and within areas of inflammation in replacement HGP CRCLMs, compared to those in desmoplastic HGP CRCLMs.

The aforementioned experiments were conducted using only replacement and desmoplastic HGP tumour specimens because the vast majority of CRCLMs present with these two growth patterns. CRCLMs that are scored as having a predominant pushing HGP are quite rare, and there were no such tissues available at the MUHC-Research Institute Liver Disease Biobank amid their chemonaïve samples.

2.4.1. Replacement HGP CRCLM gene expression signature

The criteria for the gene expression signature were designed to identify DEGs whose transcription was significantly upregulated in the replacement HGP CRCLMs, using the RNA counts for these genes in desmoplastic HGP CRCLMs and adjacent normal liver

tissues as baselines for comparison. The statistical thresholds for a DEG's inclusion were fold changes greater than 2 and *P* values less than 0.05 because these had been used in a recent study that sought to detect genes differentially expressed between primary CRCs, CRCLMs, normal colon tissues, and normal liver tissues [71]. It was unsurprising to discover that only 53 DEGs met all three conditions considering that replacement and desmoplastic HGP CRCLMs essentially arise from a common colorectal, neoplastic source. Previous studies that have compared the gene expression and gene mutation profiles of CRCs with those of their associated CRCLMs have reported high concordance rates [71,72]. Provided that the primary tumours and their corresponding liver metastases are insignificantly different at the level of transcriptomics, it is reasonable to infer that the gene expression profiles between CRCLMs that differ in growth pattern would be equally similar.

In fact, the degree of differential gene expression that was seen in the RNA-Seq data may be an overestimation due to the method by which the tissues were collected. Prior to RNA extraction, the CRCLMs were excised from sections via macrodissection, not by laser capture microdissection. Therefore, non-neoplastic cells within close proximity of the tumour-liver interface may have contributed to the total RNA that was sequenced. The criterion requiring that DEGs included in the gene expression signature be significantly upregulated in the replacement HGP tumours relative to the adjacent normal liver tissues was designed to mitigate the impact of these potential non-neoplastic inputs. Nevertheless, this highlights an important concept that must inevitably be addressed in future studies that focus on HGPs in CRCLM – cell-cell interactions between the tumour and parenchyma. Differences in the tumour cell interactions with hepatocytes, leukocytes, and stromal cells between replacement and desmoplastic HGP CRCLMs may be responsible for their distinguishable gene expression profiles.

The replacement HGP CRCLM gene expression signature does not contain a large enough number of DEGs for pathway analysis software to be particularly useful. These programs often suggested pathways on the basis of a single entity being included in the list of 53 genes. However, broad themes that were represented by multiple genes in the signature include the immune system and the extracellular matrix. Specifically, the replacement HGP CRCLM gene expression signature that was generated in this study

encompasses DEGs that encode chemokines, leukocyte markers, non-collagen ECM components, and ECM-remodelling proteins. Three of these DEGs were chosen for immunohistochemistry assay – LOXL4, CXCL6, and TNC.

2.4.2. LOXL4 staining in replacement and desmoplastic HGP CRCLMs

This study showed that LOXL4 expression is significantly upregulated in chemonaïve replacement HGP CRCLMs compared to chemonaïve desmoplastic HGP CRCLMs, both at the level of mRNA and protein. Digital image analysis of the LOXL4 IHC results revealed this increased expression of LOXL4 protein to be significant at the tumour-liver interface and in the areas of inflammation. Furthermore, the cells that were staining positive for LOXL4 were neither tumour cells nor hepatocytes. Given the morphology and location of these cells, it is highly suspected that they represent at least one of the various classes of leukocytes. Moreover, our presumptions about the identity of the LOXL4-expressing cells were supported by pathologists consulted to aid in the interpretation of these findings.

Upon the putative confirmation of these positively-stained cells' leukocytic origin, this study would be the first to show the expression of LOXL4 protein by immune cells in the context of cancer. The pro-metastatic roles of LOXL4 protein expression by HNSCC and gastric cancer cells have been discussed, in addition to a similar function attributed to spliced LOXL4 mRNA variants expressed by ovarian cancer cells [47,55,57]. While the LOXL4 mRNA that is elevated in replacement HGP CRCLMs cannot be assigned to specific cells by RNA-Seq alone, our IHC data suggest that the LOXL4 protein is not from a neoplastic source, in contrast to what has been observed in other types of cancer. Our initial suspicion is that the LOXL4-positive cells are neutrophils and/or macrophages, based on certain DEGs that were overexpressed in replacement HGP CRCLMs. CXCL6 (granulocyte chemotactic protein-2) is a potent chemoattractant for neutrophils that met the criteria for the gene expression signature [73]. While CXCL6 protein was expressed by cancer cells in both growth patterns, there may be other factors unique to the replacement HGP metastases that promote the expression of LOXL4 once neutrophils have been mobilized towards the tumour tissue. CD68, the classical marker used to identify macrophages, was also overexpressed in replacement HGP CRCLMs [74]. Therefore, a

greater quantity of Kupffer cells and/or circulating monocytes may have been recruited to these metastases, especially given that CCL2 (monocyte chemoattractant protein-1) was yet another DEG included in the gene signature. CCL2 and CXCL6 have even been shown to synergistically enhance neutrophil chemotaxis in inflammatory microenvironments and gastrointestinal malignancies [75].

This study also demonstrated that the expression of LOXL4 protein was increased in replacement HGP CRCLMs that had been treated with bev-chemo compared to desmoplastic HGP CRCLMs that underwent the same regimen. Replacement HGP CRCLMs were already known to be resistant to anti-angiogenic therapy by virtue of their vascularization being independent of VEGF [33]. Consequently, the fact that the treated replacement HGP metastases had substantially larger areas of viable tumour than the treated desmoplastic HGP lesions, in which there was extensive necrosis, was to be expected. There were relatively few detectable cells in these areas where the desmoplastic HGP CRCLMs had developed prior to their treatment with bev-chemo, let alone any that stained positive for LOXL4. Meanwhile, there were numerous LOXL4-expressing cells at the tumour-liver interface, as well as within the tumour stroma and areas of tumour necrosis in the replacement HGP CRCLMs, which mostly withstood treatment. Our current data are not sufficient to determine whether there is a causal relationship between LOXL4 protein expression and resistance to bev-chemo in CRCLM. Nevertheless, studies have reported that the LOX family of enzymes can confer resistance to chemotherapy through their ECM-modifying function. Collagen stabilization via LOX-catalyzed crosslinking can limit the transport of anti-cancer drugs to the tumour, in addition to their diffusion within it thereafter [76,77].

2.4.3. EV-based liquid biopsy in CRCLM

In this study, we successfully isolated EVs from the plasma of chemonaïve patients with CRCLM or benign liver disease via differential centrifugation. The enrichment of particles measuring less than 1000 nm in diameter was confirmed by NTA, and follow-up immunoblotting of these pelleted vesicles revealed that all samples were positive for the EV markers CD81/TAPA-1 and TSG101. We then sought to investigate whether there were any differences in the levels of putative EV-derived LOXL4 protein between patients

with replacement HGP CRCLM, desmoplastic HGP CRCLM, and benign liver disease. LOXL4 was prioritized for EV-based protein detection due to our immunohistochemical findings, as well as there being evidence of EV-associated lysyl oxidases in the context of hypoxia and cancer [78,79].

LOXL4 protein was detected in the EVs from all the patients whose plasma had been collected for this study. The banding pattern was consistent across the three categories of patients, with multiple bands appearing in every case. A possible explanation for this finding would be that these bands represent the protein products of LOXL4 spliced variant mRNAs, which have been shown to be transcribed in ovarian cancer, breast cancer, and malignant mesothelioma [56,57]. Alternatively, the observed banding pattern may also be the consequence of the antibody that was used for Western blotting, considering that it had not been approved for this technique. A repeat experiment using a more suitable antibody may be warranted to assess the validity of the EV-derived LOXL4 protein detection results.

Nonetheless, the absence of differential EV-associated LOXL4 protein levels in the plasma of patients with either CRCLM or benign liver disease may be attributed to the fact that normal tissues also express LOXL4. A method that would allow for the isolation of EVs that are released by specific cell types of interest could potentially be used to eliminate this background effect. The use of CD326 (EpCAM) MicroBeads is one way of positively selecting for EVs released from epithelial tumour cells [80,81]. EpCAM immunostaining was performed on chemonaïve replacement HGP CRCLMs, chemonaïve desmoplastic HGP CRCLMs, and specimens of benign liver disease as a proof of concept for the applicability of these microbeads. The expression of EpCAM protein was found to be specific to the tumour cells and cholangiocytes, with the former comprising the vast majority of the positively-stained cells. However, a trial run for EV isolation from the plasma of the same patients using the CD326 (EpCAM) MicroBeads proved unsuccessful because there were no detectable bands for either the EV markers or LOXL4.

Limitations

Although this study had been thoroughly designed, there remain limitations that must be acknowledged. First, the RNA-Seq data used to generate the gene expression signature, and to subsequently select targets for protein detection, were derived from a small sample size of resected tumours. It is rather uncommon to identify patients with CRCLM who are considered resectable despite never having been exposed to chemotherapy, hence the limited access to these tissues. Additional chemonaïve CRCLMs could be acquired and included in the study to bolster the sample size, either by prospectively sequencing new chemonaïve liver metastases resected at the MUHC or through collaborations with other hospital centres. Furthermore, it would be interesting to evaluate the gene expression profiles of replacement and desmoplastic CRCLMs that have been treated either with chemotherapy alone, or with bev-chemo. Second, the short supply of chemonaïve CRCLM tissues, in addition to the manual nature of the IHC performed in this study, made it such that only three of the DEGs in the gene expression signature were chosen for staining. Provided supplementary resources, the protein expression patterns of many more of these genes whose transcription was significantly upregulated in replacement HGP metastases could be examined. Lastly, the results obtained in this study were primarily morphological. Therefore, there is a compelling opportunity to build upon the discovery of differentially expressed gene products enriched in replacement HGP CRCLMs through molecular and functional analyses. For example, future studies can investigate pathways that are involved in the differential expression of these DEGs, or evaluate the functional importance of LOXL4 in the development of replacement HGP metastases.

Conclusion

The gene expression profiles of chemonaïve colorectal cancer liver metastases that differ in their predominant histopathological growth pattern were evaluated. Several genes which are upregulated in the replacement HGP metastases compared to the desmoplastic HGP metastases and normal liver tissues are associated with the extracellular matrix and the immune system.

In addition to being transcriptionally upregulated in the chemonaïve replacement HGP CRCLMs, the levels of LOXL4 protein were significantly elevated in replacement HGP metastases, notably at the tumour-liver interface and within areas of inflammation. The LOXL4-expressing cells were neither tumour cells nor hepatocytes in the replacement and desmoplastic CRCLMs. They are highly suspected to be leukocytes, though the precise identification of these LOXL4-positive cell types requires further investigation. The association between replacement HGP metastases and increased expression of LOXL4 protein was consistent in tumours that had been treated with bevacizumab plus chemotherapy.

LOXL4 was also detected in extracellular vesicles isolated from the plasma of patients with CRCLM or benign liver disease. Methods which allow for the isolation of EVs specific to certain cell types, such as leukocytes or tumour cells, may be necessary to determine whether LOXL4 can be used as a biomarker in EV-based liquid biopsies to distinguish between the growth patterns in CRCLM.

Bibliography

1. Canadian Cancer Society's Advisory Committee on Cancer Statistics. Canadian Cancer Statistics 2017 [Internet]. Toronto, ON: Canadian Cancer Society; 2017 [cited 2018 July 1]. Available from: cancer.ca/Canadian-Cancer- Statistics-2017-EN.pdf.
2. Siegel RL, Miller KD, Jemal A. Cancer Statistics, 2017. CA Cancer J Clin. 2017;67(1):7-30.
3. Siegel RL, Miller KD, Fedewa SA, Ahnen DJ, Meester RGS, Barzi A, et al. Colorectal cancer statistics, 2017. CA Cancer J Clin. 2017;67(3):177-93.
4. Brenner H, Kloor M, Pox CP. Colorectal cancer. Lancet. 2014;383(9927):1490-502.
5. Cappell MS. From colonic polyps to colon cancer: pathophysiology, clinical presentation, and diagnosis. Clin Lab Med. 2005;25(1):135-77.
6. Cappell MS. Pathophysiology, clinical presentation, and management of colon cancer. Gastroenterol Clin North Am. 2008;37(1):1-24, v.
7. National Institute for Health and Care Excellence (NICE), *Colorectal cancer: diagnosis and management [CG131]*. 2011. Available from: https://www.nice.org.uk/guidance/cg131 [Accessed 23 July 2018].
8. Poston GJ, Tait D, O'Connell S, Bennett A, Berendse S, Guideline Development G. Diagnosis and management of colorectal cancer: summary of NICE guidance. BMJ. 2011;343:d6751.
9. Brierley JD, Gospodarowicz MK, Wittekind C, O'Sullivan B, Mason M, Asamura H et al., editors. *TNM classification of malignant tumours*. 8th ed. Oxford: John Wiley & Sons, Inc.; 2017.
10. van Gijn W, Marijnen CA, Nagtegaal ID, Kranenbarg EM, Putter H, Wiggers T, et al. Preoperative radiotherapy combined with total mesorectal excision for resectable rectal cancer: 12-year follow-up of the multicentre, randomised controlled TME trial. Lancet Oncol. 2011;12(6):575-82.
11. Hofheinz RD, Wenz F, Post S, Matzdorff A, Laechelt S, Hartmann JT, et al. Chemoradiotherapy with capecitabine versus fluorouracil for locally advanced rectal cancer: a randomised, multicentre, non-inferiority, phase 3 trial. Lancet Oncol. 2012;13(6):579-88.
12. Andre T, Boni C, Navarro M, Tabernero J, Hickish T, Topham C, et al. Improved overall survival with oxaliplatin, fluorouracil, and leucovorin as adjuvant treatment in stage II or III colon cancer in the MOSAIC trial. J Clin Oncol. 2009;27(19):3109-16.
13. Haller DG, Tabernero J, Maroun J, de Braud F, Price T, Van Cutsem E, et al. Capecitabine plus oxaliplatin compared with fluorouracil and folinic acid as adjuvant therapy for stage III colon cancer. J Clin Oncol. 2011;29(11):1465-71.
14. Amaro A, Chiara S, Pfeffer U. Molecular evolution of colorectal cancer: from multistep carcinogenesis to the big bang. Cancer Metastasis Rev. 2016;35(1):63-74.
15. Leddin DJ, Enns R, Hilsden R, Plourde V, Rabeneck L, Sadowski DC, et al. Canadian Association of Gastroenterology position statement on screening individuals at average risk for developing colorectal cancer: 2010. Can J Gastroenterol. 2010;24(12):705-14.
16. Bacchus CM, Dunfield L, Gorber SC, Holmes NM, Birtwhistle R, Dickinson JA, et al. Recommendations on screening for colorectal cancer in primary care. CMAJ. 2016;188(5):340-8.

17. Leddin D, Hunt R, Champion M, Cockeram A, Flook N, Gould M, et al. Canadian Association of Gastroenterology and the Canadian Digestive Health Foundation: Guidelines on colon cancer screening. Can J Gastroenterol. 2004;18(2):93-9.
18. Bird NC, Mangnall D, Majeed AW. Biology of colorectal liver metastases: A review. J Surg Oncol. 2006;94(1):68-80.
19. Choti MA, Sitzmann JV, Tiburi MF, Sumetchotimetha W, Rangsin R, Schulick RD, et al. Trends in long-term survival following liver resection for hepatic colorectal metastases. Ann Surg. 2002;235(6):759-66.
20. Abdalla EK, Vauthey JN, Ellis LM, Ellis V, Pollock R, Broglio KR, et al. Recurrence and outcomes following hepatic resection, radiofrequency ablation, and combined resection/ablation for colorectal liver metastases. Ann Surg. 2004;239(6):818-25; discussion 25-7.
21. Abdalla EK, Adam R, Bilchik AJ, Jaeck D, Vauthey JN, Mahvi D. Improving resectability of hepatic colorectal metastases: expert consensus statement. Ann Surg Oncol. 2006;13(10):1271-80.
22. Berri RN, Abdalla EK. Curable metastatic colorectal cancer: recommended paradigms. Curr Oncol Rep. 2009;11(3):200-8.
23. Fakih MG. Metastatic colorectal cancer: current state and future directions. J Clin Oncol. 2015;33(16):1809-24.
24. Vermeulen PB, Colpaert C, Salgado R, Royers R, Hellemans H, Van Den Heuvel E, et al. Liver metastases from colorectal adenocarcinomas grow in three patterns with different angiogenesis and desmoplasia. J Pathol. 2001;195(3):336-42.
25. Van den Eynden GG, Majeed AW, Illemann M, Vermeulen PB, Bird NC, Hoyer-Hansen G, et al. The multifaceted role of the microenvironment in liver metastasis: biology and clinical implications. Cancer Res. 2013;73(7):2031-43.
26. van Dam PJ, van der Stok EP, Teuwen LA, Van den Eynden GG, Illemann M, Frentzas S, et al. International consensus guidelines for scoring the histopathological growth patterns of liver metastasis. Br J Cancer. 2017;117(10):1427-41.
27. Ohlsson B, Stenram U, Tranberg KG. Resection of colorectal liver metastases: 25-year experience. World J Surg. 1998;22(3):268-76; discussion 76-7.
28. Lunevicius R, Nakanishi H, Ito S, Kozaki K, Kato T, Tatematsu M, et al. Clinicopathological significance of fibrotic capsule formation around liver metastasis from colorectal cancer. J Cancer Res Clin Oncol. 2001;127(3):193-9.
29. Nielsen K, Rolff HC, Eefsen RL, Vainer B. The morphological growth patterns of colorectal liver metastases are prognostic for overall survival. Mod Pathol. 2014;27(12):1641-8.
30. Eefsen RL, Vermeulen PB, Christensen IJ, Laerum OD, Mogensen MB, Rolff HC, et al. Growth pattern of colorectal liver metastasis as a marker of recurrence risk. Clin Exp Metastasis. 2015;32(4):369-81.
31. Van den Eynden GG, Bird NC, Majeed AW, Van Laere S, Dirix LY, Vermeulen PB. The histological growth pattern of colorectal cancer liver metastases has prognostic value. Clin Exp Metastasis. 2012;29(6):541-9.
32. Lazaris A, Amri A, Petrillo SK, Zoroquiain P, Ibrahim N, Salman A, et al. Vascularization of colorectal carcinoma liver metastasis: insight into stratification of patients for anti-angiogenic therapies. J Pathol Clin Res. 2018.

33. Frentzas S, Simoneau E, Bridgeman VL, Vermeulen PB, Foo S, Kostaras E, et al. Vessel co-option mediates resistance to anti-angiogenic therapy in liver metastases. Nat Med. 2016;22(11):1294-302.
34. Csiszar K. Lysyl oxidases: a novel multifunctional amine oxidase family. Prog Nucleic Acid Res Mol Biol. 2001;70:1-32.
35. Barker HE, Cox TR, Erler JT. The rationale for targeting the LOX family in cancer. Nat Rev Cancer. 2012;12(8):540-52.
36. Thomassin L, Werneck CC, Broekelmann TJ, Gleyzal C, Hornstra IK, Mecham RP, et al. The Pro-regions of lysyl oxidase and lysyl oxidase-like 1 are required for deposition onto elastic fibers. J Biol Chem. 2005;280(52):42848-55.
37. Hohenester E, Sasaki T, Timpl R. Crystal structure of a scavenger receptor cysteine-rich domain sheds light on an ancient superfamily. Nat Struct Biol. 1999;6(3):228-32.
38. Liu Y, Cao X. Characteristics and Significance of the Pre-metastatic Niche. Cancer Cell. 2016;30(5):668-81.
39. Chin AR, Wang SE. Cancer Tills the Premetastatic Field: Mechanistic Basis and Clinical Implications. Clin Cancer Res. 2016;22(15):3725-33.
40. Erler JT, Bennewith KL, Nicolau M, Dornhofer N, Kong C, Le QT, et al. Lysyl oxidase is essential for hypoxia-induced metastasis. Nature. 2006;440(7088):1222-6.
41. Erler JT, Bennewith KL, Cox TR, Lang G, Bird D, Koong A, et al. Hypoxia-induced lysyl oxidase is a critical mediator of bone marrow cell recruitment to form the premetastatic niche. Cancer Cell. 2009;15(1):35-44.
42. Cox TR, Bird D, Baker AM, Barker HE, Ho MW, Lang G, et al. LOX-mediated collagen crosslinking is responsible for fibrosis-enhanced metastasis. Cancer Res. 2013;73(6):1721-32.
43. Cox TR, Gartland A, Erler JT. Lysyl Oxidase, a Targetable Secreted Molecule Involved in Cancer Metastasis. Cancer Res. 2016;76(2):188-92.
44. Cox TR, Rumney RMH, Schoof EM, Perryman L, Hoye AM, Agrawal A, et al. The hypoxic cancer secretome induces pre-metastatic bone lesions through lysyl oxidase. Nature. 2015;522(7554):106-10.
45. Maki JM, Tikkanen H, Kivirikko KI. Cloning and characterization of a fifth human lysyl oxidase isoenzyme: the third member of the lysyl oxidase-related subfamily with four scavenger receptor cysteine-rich domains. Matrix Biol. 2001;20(7):493-6.
46. Holtmeier C, Gorogh T, Beier U, Meyer J, Hoffmann M, Gottschlich S, et al. Overexpression of a novel lysyl oxidase-like gene in human head and neck squamous cell carcinomas. Anticancer Res. 2003;23(3B):2585-91.
47. Gorogh T, Weise JB, Holtmeier C, Rudolph P, Hedderich J, Gottschlich S, et al. Selective upregulation and amplification of the lysyl oxidase like-4 (LOXL4) gene in head and neck squamous cell carcinoma. J Pathol. 2007;212(1):74-82.
48. Weise JB, Rudolph P, Heiser A, Kruse ML, Hedderich J, Cordes C, et al. LOXL4 is a selectively expressed candidate diagnostic antigen in head and neck cancer. Eur J Cancer. 2008;44(9):1323-31.
49. Gorogh T, Quabius ES, Heidebrecht H, Nagy A, Muffels T, Haag J, et al. Lysyl oxidase like-4 monoclonal antibody demonstrates therapeutic effect against head and neck squamous cell carcinoma cells and xenografts. Int J Cancer. 2016;138(10):2529-38.

50. Weise JB, Csiszar K, Gottschlich S, Hoffmann M, Schmidt A, Weingartz U, et al. Vaccination strategy to target lysyl oxidase-like 4 in dendritic cell based immunotherapy for head and neck cancer. Int J Oncol. 2008;32(2):317-22.
51. Wu G, Guo Z, Chang X, Kim MS, Nagpal JK, Liu J, et al. LOXL1 and LOXL4 are epigenetically silenced and can inhibit ras/extracellular signal-regulated kinase signaling pathway in human bladder cancer. Cancer Res. 2007;67(9):4123-9.
52. Kim DJ, Lee DC, Yang SJ, Lee JJ, Bae EM, Kim DM, et al. Lysyl oxidase like 4, a novel target gene of TGF-beta1 signaling, can negatively regulate TGF-beta1-induced cell motility in PLC/PRF/5 hepatoma cells. Biochem Biophys Res Commun. 2008;373(4):521-7.
53. Busnadiego O, Gonzalez-Santamaria J, Lagares D, Guinea-Viniegra J, Pichol-Thievend C, Muller L, et al. LOXL4 is induced by transforming growth factor beta1 through Smad and JunB/Fra2 and contributes to vascular matrix remodeling. Mol Cell Biol. 2013;33(12):2388-401.
54. Tian M, Liu W, Jin L, Jiang X, Yang L, Ding Z, et al. LOXL4 is downregulated in hepatocellular carcinoma with a favorable prognosis. Int J Clin Exp Pathol. 2015;8(4):3892-900.
55. Li RK, Zhao WY, Fang F, Zhuang C, Zhang XX, Yang XM, et al. Lysyl oxidase-like 4 (LOXL4) promotes proliferation and metastasis of gastric cancer via FAK/Src pathway. J Cancer Res Clin Oncol. 2015;141(2):269-81.
56. Sebban S, Davidson B, Reich R. Lysyl oxidase-like 4 is alternatively spliced in an anatomic site-specific manner in tumors involving the serosal cavities. Virchows Arch. 2009;454(1):71-9.
57. Sebban S, Golan-Gerstl R, Karni R, Vaksman O, Davidson B, Reich R. Alternatively spliced lysyl oxidase-like 4 isoforms have a pro-metastatic role in cancer. Clin Exp Metastasis. 2013;30(1):103-17.
58. Raposo G, Stoorvogel W. Extracellular vesicles: exosomes, microvesicles, and friends. J Cell Biol. 2013;200(4):373-83.
59. Xu R, Greening DW, Zhu HJ, Takahashi N, Simpson RJ. Extracellular vesicle isolation and characterization: toward clinical application. J Clin Invest. 2016;126(4):1152-62.
60. Kalluri R. The biology and function of exosomes in cancer. J Clin Invest. 2016;126(4):1208-15.
61. Clayton A, Mason MD. Exosomes in tumour immunity. Curr Oncol. 2009;16(3):46-9.
62. Greening DW, Gopal SK, Xu R, Simpson RJ, Chen W. Exosomes and their roles in immune regulation and cancer. Semin Cell Dev Biol. 2015;40:72-81.
63. Ribeiro MF, Zhu H, Millard RW, Fan GC. Exosomes Function in Pro- and Anti-Angiogenesis. Curr Angiogenes. 2013;2(1):54-9.
64. Kucharzewska P, Christianson HC, Welch JE, Svensson KJ, Fredlund E, Ringner M, et al. Exosomes reflect the hypoxic status of glioma cells and mediate hypoxia-dependent activation of vascular cells during tumor development. Proc Natl Acad Sci U S A. 2013;110(18):7312-7.
65. Becker A, Thakur BK, Weiss JM, Kim HS, Peinado H, Lyden D. Extracellular vesicles in cancer: cell-to-cell mediators of metastasis. Cancer Cell. 2016;30(6):836-48.
66. Hoshino A, Costa-Silva B, Shen TL, Rodrigues G, Hashimoto A, Tesic Mark M, et al. Tumour exosome integrins determine organotropic metastasis. Nature. 2015;527(7578):329-35.

67. Siravegna G, Marsoni S, Siena S, Bardelli A. Integrating liquid biopsies into the management of cancer. Nat Rev Clin Oncol. 2017;14(9):531-48.
68. Kahlert C, Melo SA, Protopopov A, Tang J, Seth S, Koch M, et al. Identification of double-stranded genomic DNA spanning all chromosomes with mutated KRAS and p53 DNA in the serum exosomes of patients with pancreatic cancer. J Biol Chem. 2014;289(7):3869-75.
69. Thakur BK, Zhang H, Becker A, Matei I, Huang Y, Costa-Silva B, et al. Double-stranded DNA in exosomes: a novel biomarker in cancer detection. Cell Res. 2014;24(6):766-9.
70. Ogata-Kawata H, Izumiya M, Kurioka D, Honma Y, Yamada Y, Furuta K, et al. Circulating exosomal microRNAs as biomarkers of colon cancer. PLoS One. 2014;9(4):e92921.
71. Lee JR, Kwon CH, Choi Y, Park HJ, Kim HS, Jo HJ, et al. Transcriptome analysis of paired primary colorectal carcinoma and liver metastases reveals fusion transcripts and similar gene expression profiles in primary carcinoma and liver metastases. BMC Cancer. 2016;16:539.
72. Lim B, Mun J, Kim JH, Kim CW, Roh SA, Cho DH, et al. Genome-wide mutation profiles of colorectal tumors and associated liver metastases at the exome and transcriptome levels. Oncotarget. 2015;6(26):22179-90.
73. Proost P, De Wolf-Peeters C, Conings R, Opdenakker G, Billiau A, Van Damme J. Identification of a novel granulocyte chemotactic protein (GCP-2) from human tumor cells. In vitro and in vivo comparison with natural forms of GRO, IP-10, and IL-8. J Immunol. 1993;150(3):1000-10.
74. Strauss O, Dunbar PR, Bartlett A, Phillips A. The immunophenotype of antigen presenting cells of the mononuclear phagocyte system in normal human liver--a systematic review. J Hepatol. 2015;62(2):458-68.
75. Gijsbers K, Gouwy M, Struyf S, Wuyts A, Proost P, Opdenakker G, et al. GCP-2/CXCL6 synergizes with other endothelial cell-derived chemokines in neutrophil mobilization and is associated with angiogenesis in gastrointestinal tumors. Exp Cell Res. 2005;303(2):331-42.
76. Rossow L, Veitl S, Vorlova S, Wax JK, Kuhn AE, Maltzahn V, et al. LOX-catalyzed collagen stabilization is a proximal cause for intrinsic resistance to chemotherapy. Oncogene. 2018.
77. Le Calve B, Griveau A, Vindrieux D, Marechal R, Wiel C, Svrcek M, et al. Lysyl oxidase family activity promotes resistance of pancreatic ductal adenocarcinoma to chemotherapy by limiting the intratumoral anticancer drug distribution. Oncotarget. 2016;7(22):32100-12.
78. Kucharzewska P, Christianson HC, Welch JE, Svensson KJ, Fredlund E, Ringner M, et al. Exosomes reflect the hypoxic status of glioma cells and mediate hypoxia-dependent activation of vascular cells during tumor development. Proc Natl Acad Sci U S A. 2013;110(18):7312-7.
79. de Jong OG, van Balkom BW, Gremmels H, Verhaar MC. Exosomes from hypoxic endothelial cells have increased collagen crosslinking activity through up-regulation of lysyl oxidase-like 2. J Cell Mol Med. 2016;20(2):342-50.
80. Tauro BJ, Greening DW, Mathias RA, Ji H, Mathivanan S, Scott AM, et al. Comparison of ultracentrifugation, density gradient separation, and immunoaffinity capture methods for isolating human colon cancer cell line LIM1863-derived exosomes. Methods. 2012;56(2):293-304.
81. Taylor DD, Gercel-Taylor C. MicroRNA signatures of tumor-derived exosomes as diagnostic biomarkers of ovarian cancer. Gynecol Oncol. 2008;110(1):13-21.

Appendix

Supplementary Methods

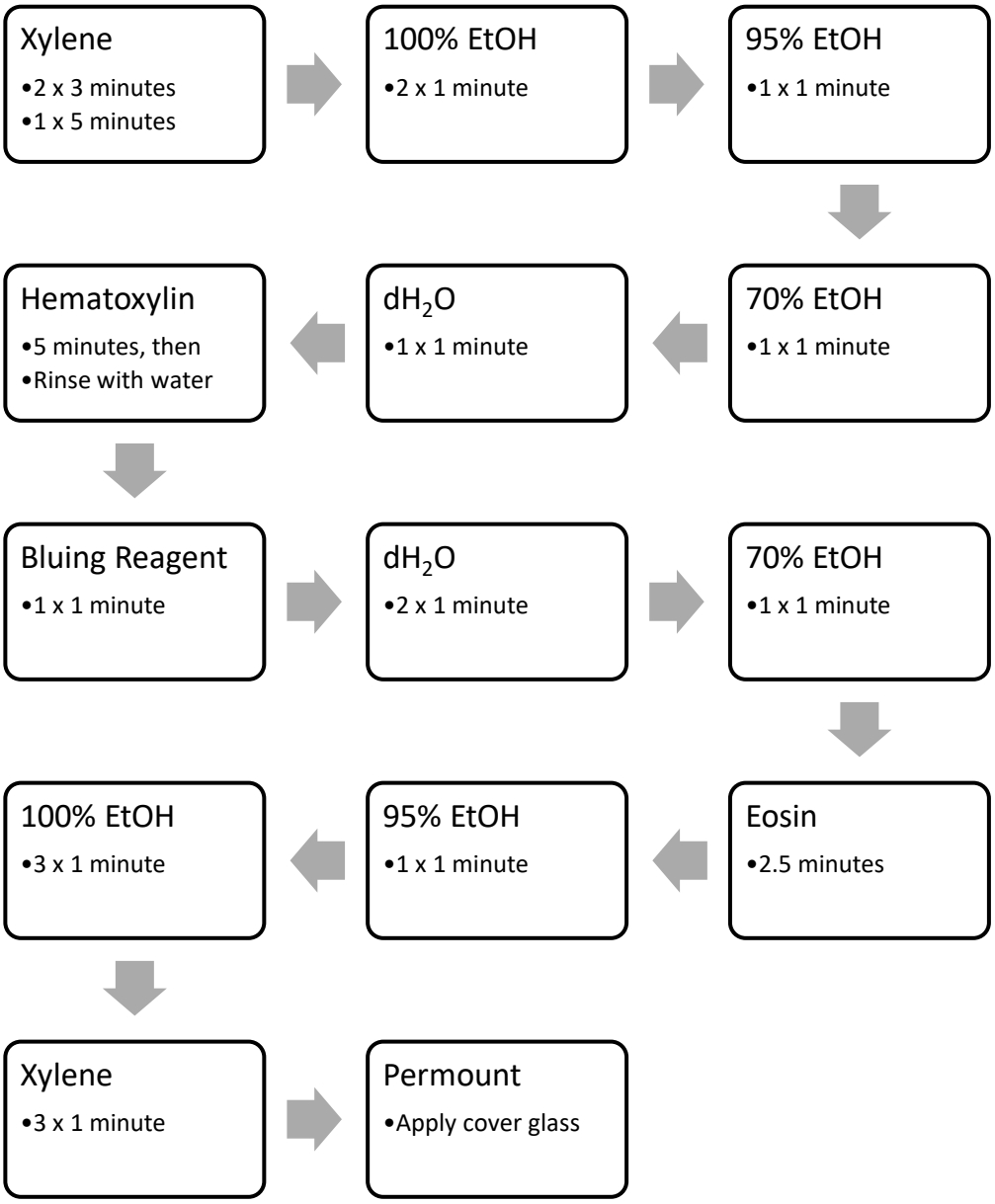

Figure 12: Flow diagram of the H&E staining protocol [2.2.4.]

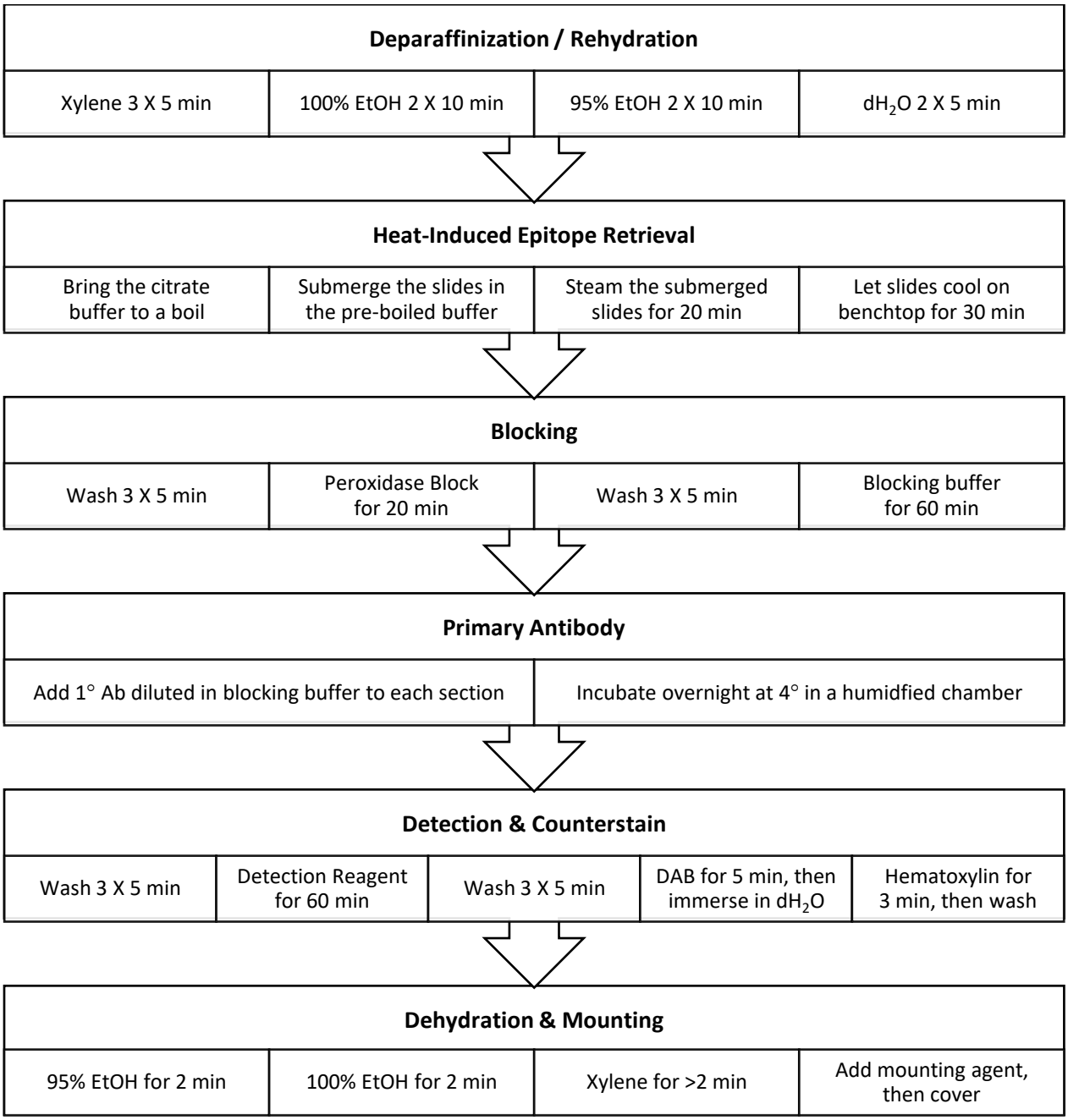

Figure 13: Flow diagram of the immunohistochemistry protocol [2.2.5.]

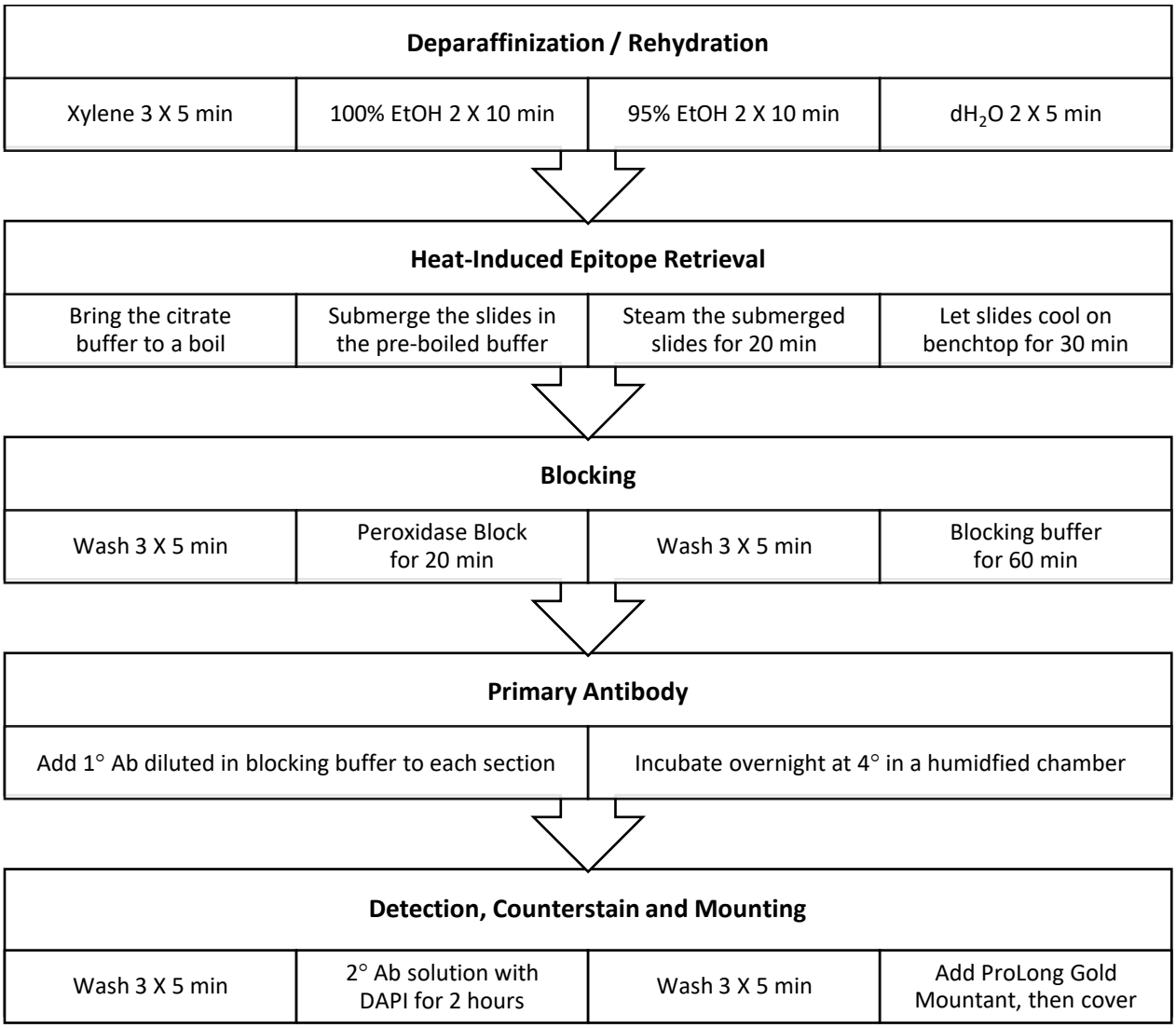

Figure 14: Flow diagram of the immunofluorescence protocol [2.2.6.]

Supplementary Tables

Gene ID	Average RHGP Counts	Fold Change RT vs RN	*P*-Values RN vs RT	Fold Change RT vs DT	*P*-Values DT vs RT
CXCL6	1047.5	5.513157895	0.00743703	8.810747664	0.000496632
PTHLH	180.666667	120.4444444	1.3781E-05	3.662162162	0.000500025
LOXL4	408.666667	6.239185751	0.00770154	5.555891239	0.001458219
RRAD	166.833333	15.16666667	0.00412909	5.142123288	0.003120909
TNC	4106	34.12188366	0.00197669	3.804983526	0.004968071
ANKRD1	164.666667	8.900900901	0.00857325	4.689873418	0.007457654
RASA3	1464.83333	20.43953488	0.01158793	4.528856063	0.00902489
HRCT1	128.333333	15.71428571	0.0018879	2.5	0.009569991
TUBAL3	203.5	#DIV/0!	0.01066832	5.073407202	0.010188227
SPIRE1	791.333333	5.383219955	0.01473349	3.033219761	0.010644214
PDZD3	257.666667	309.2	9.9976E-05	2.380903491	0.01076699
DCDC2	722.333333	9.401301518	0.02310859	5.319967267	0.01138321
FAM40B	133	38	5.3089E-05	2.049657534	0.011761667
TFF1	1959.66667	75.37179487	0.01576664	5.33969119	0.011963637
SDR16C5	357.166667	535.75	0.02013983	7.175223214	0.012673443
CAPN2	7638.16667	9.459029928	0.00098624	2.161541364	0.015121779
CD72	163.166667	3.534296029	0.01216769	2.231762918	0.015335487
CCNJL	199.166667	38.5483871	0.00044481	2.327922078	0.016711185
OLR1	1133	61.8	0.0077654	3.405811623	0.01672124
CDC42EP2	393.333333	7.421383648	0.00123506	2.027491409	0.016790892
ITIH5	518	14.72985782	0.02258366	5.321917808	0.016915574
SNCAIP	216.333333	12.13084112	0.00926573	3.585635359	0.017018904
DUOXA2	505.666667	65.95652174	0.03772141	10.06858407	0.017716542
TIMP3	8686.5	4.732068277	0.01776985	3.045045571	0.018158846
CRLF1	182	78	0.02108303	5.352941176	0.020087594
WSCD1	140.333333	8.42	0.01761206	3.118518519	0.022600065
SLC6A20	826	154.875	0.0364665	7.039772727	0.023258684
TMEM92	269.666667	5.758007117	0.02651057	2.924096386	0.023477632
ITPKA	214.333333	44.34482759	0.00053096	2.293697979	0.023747045
FHL3	407.833333	7.670846395	0.00646036	2.249080882	0.025875344
FNDC1	1689.66667	153.6060606	0.00452146	2.828683036	0.026780407
ECM1	1308.83333	3.190979277	0.03161854	2.414326706	0.027551508
MAP9	231.166667	9.767605634	0.01023806	2.660485934	0.029520061
LBH	2416.33333	16.12680756	0.0006331	2.148276203	0.03209431
KIT	310.166667	8.271111111	0.00189345	2.127667683	0.032147648

CCL2	1485.33333	2.769422001	0.01706608	2.458256712	0.032299511
DNAJB5	167	2.700808625	0.02187898	2.119887165	0.032367293
RHOF	878.833333	39.05925926	0.00678117	2.934879406	0.03237795
PTPRR	1088.83333	272.2083333	0.00776966	2.893268379	0.033092237
PMP22	2246	14.89060773	0.00345471	2.087360595	0.03335367
KLK10	1508.66667	348.1538462	0.04948519	7.505804312	0.033591057
APOBR	695.666667	22.32085561	0.00906072	2.636210526	0.036118503
MEX3B	153.833333	20.97727273	0.01496348	2.774549098	0.037555055
CRYAB	331.333333	4.677647059	0.02807141	2.442260442	0.039654266
GPRC5B	375.166667	4.207476636	0.03484866	2.4808964	0.040217568
HSPB8	332.166667	5.931547619	0.01694138	2.426542208	0.040754543
NPTX1	227.833333	170.875	0.03251509	4.227835052	0.041706337
PTGS1	571.333333	10.08235294	0.01503568	2.513196481	0.042266149
MYZAP	219.333333	14	0.00066011	2.016343207	0.043243693
CD68	4162.16667	4.493971567	0.01832691	2.291941997	0.043746345
FSTL3	1725.16667	14.0067659	0.01096153	2.725860253	0.046583231
FGD5	516.5	6.298780488	0.0094937	2.276444662	0.048555755
BTNL8	190.166667	18.40322581	0.01183961	2.742788462	0.049977899

Table 1: RNA-Seq data for the differentially expressed genes constituting the replacement CRCLM gene expression signature. RHGP, replacement HGP; RT, replacement HGP tumour; RN, normal liver adjacent to replacement HGP tumour; DT, desmoplastic HGP tumour.